



Pharmacodynamics of Moxifloxacin, Meropenem, Caspofungin, and Their Combinations against *In Vitro* Polymicrobial Interkingdom Biofilms

Albert Ruiz-Sorribas,^a Hervé Poilvache,^{b,c} Françoise Van Bambeke^a

^aPharmacologie cellulaire et moléculaire, Louvain Drug Research Institute, Université catholique de Louvain, Brussels, Belgium

^bLaboratoire de Neuro Musculo Squelettique, Institut de Recherche Expérimentale et Clinique, Université catholique de Louvain, Brussels, Belgium

^cOrthopaedic Surgery Department, Cliniques Universitaires Saint-Luc, Brussels, Belgium

ABSTRACT Biofilms colonize medical devices and are often recalcitrant to antibiotics. Interkingdom biofilms, where at least a bacterium and a fungus are present, increase the likelihood of therapeutic failures. In this work, a three-species *in vitro* biofilm model including *Staphylococcus aureus*, *Escherichia coli*, and *Candida albicans* was used to study the activity of the antibiotics moxifloxacin and meropenem, the antifungal caspofungin, and combinations of them against interkingdom biofilms. The culturable cells and total biomass were evaluated to determine the pharmacodynamic parameters of the drug response for the incubation with the drugs alone. The synergic or antagonistic effects (increased/decreased effects) of the combination of drugs were analyzed with the highest-single-agent method. Biofilms were imaged in confocal microscopy after live/dead staining. The drugs had limited activity when used alone against single-, dual-, and three-species biofilms. When used in combination, additive effects against single- and dual-species biofilms and increased effects (synergy) against biomass of three-species biofilms were observed. In addition, the two antibiotics showed different patterns, moxifloxacin being more active when targeting *S. aureus* and meropenem when targeting *E. coli*. All these observations were confirmed by confocal microscopy images. Our findings highlight the interest in combining caspofungin with antibiotics against interkingdom biofilms.

KEYWORDS biofilm, moxifloxacin, meropenem, caspofungin, combination, 96-well plate, *Candida albicans*, *Escherichia coli*, *Staphylococcus aureus*, antimicrobial combinations

Biofilms are consortia of microorganisms embedded in matrix produced by themselves or by the host. They can grow attached to biotic or abiotic surfaces or in aggregates (1). They are recalcitrant to antibiotics and immune defenses for several reasons. First, the matrix is a barrier that reduces the diffusion and bioavailability of drugs (2) as well as access by immune cells. Second, the scarcity of nutrients and oxygen in the biofilm triggers the appearance of dormant phenotypes. These cells with low metabolic levels are not responsive to antibiotics requiring active metabolism and replication to exert their antimicrobial effects (3). Last, dormant microorganisms surviving antibiotic exposure may regain functional metabolism and act as a reservoir, explaining relapses of the infection (4).

Medical devices are particularly prone to colonization by biofilms, i.e., vascular or urinary catheters, cardiac valves, urethral stents, endotracheal tubes, joint prostheses, etc. (1, 5). Treatment failure is frequent for such infections, leading to chronic or relapsing infections, bloodstream infection, and, in the most severe cases, death (6). A recent CDC report mentions that medical devices related infections are also associated with higher rates of antimicrobial resistance (7).

Copyright © 2022 American Society for Microbiology. All Rights Reserved.

Address correspondence to Françoise Van Bambeke, francoise.vanbambeke@uclouvain.be.

The authors declare no conflict of interest.

Received 10 November 2021

Accepted 9 December 2021

Accepted manuscript posted online 20 December 2021

Published 15 February 2022

Biofilm-associated infections of medical devices are often caused by opportunistic or nosocomial pathogens like *Staphylococcus aureus*, coagulase-negative staphylococci, *Enterobacteriaceae*, *Pseudomonas* spp., *Streptococcus* spp., and *Candida* spp. (7, 8). Fungi have a higher prevalence in culture-negative cases, i.e., patients showing symptoms of infection in the absence of isolated pathogens (9, 10). In this context, polymicrobial infections, in which at least two different pathogens are identified at the same site of infection, and more particularly interkingdom biofilms, with at least a bacterium and a fungus, are more recalcitrant and require longer treatments (11–13). A retrospective clinical study (14) showed that the failure rate for treatments of polymicrobial biofilms on prosthetic joint infections was 50.2%, compared to 31.5% for monomicrobial infections and 30.2% for culture-negative infections.

Many studies have explored the relationship between dual-species interkingdom biofilms and antimicrobial therapies (see reference 15 for a review). For example, the activity of vancomycin was reduced against *S. aureus* in coculture with *Candida albicans* due to a protective effect of the secreted fungal polysaccharides against the antibiotic action (16, 17). In the same line, mixed-species biofilms of *Staphylococcus epidermidis* and *C. albicans* were less responsive to vancomycin and fluconazole than the corresponding single-species biofilms (18). This phenomenon is also observed in mixed-species biofilms involving Gram-negative bacteria, with ofloxacin proving less active against *Escherichia coli* cocultured with *C. albicans* (19).

In this study, a previously established *in vitro* three-species biofilm model (20) was used to explore the pharmacodynamics of the combinations of a broad-spectrum antibiotic and an antifungal agent. The model includes *S. aureus* as the most frequently isolated pathogen in infections developing on orthopedic devices (1), *E. coli* as a model for *Enterobacteriaceae* (21) and *C. albicans* as a model for fungal infections (22). As broad-spectrum antibiotics, we used the fluoroquinolone moxifloxacin, which is part of the gold standard treatment for bacterial infections associated with medical devices, and the carbapenem meropenem, as a potent alternative against extended-spectrum- β -lactamase (ESBL)-producing Gram-negative bacteria, which are often coresistant to fluoroquinolones (23, 24). As an antifungal agent, the echinocandin caspofungin was tested. It is a noncompetitive inhibitor of the β -1,3-glucan synthase Gsc1 in *Candida* spp. This transmembrane enzyme adds glucose residues to the β -1,3-glucan, one of the major cell wall polysaccharides (25, 26). Gsc1 is homologous to the bacterial poly- β -1,6-*N*-acetylglucosamine (PNAG) synthases IcaA in *Staphylococcus* spp. and PgaC in *Enterobacteriaceae* (see Fig. S1 in the supplemental material). These enzymes are responsible for the elongation of the chains of PNAG, a major polysaccharidic component of the matrix (27, 28). Caspofungin and another echinocandin, anidulafungin, were shown to also target the staphylococcal enzyme, reducing the amount of PNAG in the biofilm matrix and improving the activity of antibiotics, including fluoroquinolones, against *S. aureus* biofilms (29, 30). Likewise, micafungin can potentiate the effect of levofloxacin and ceftazidime against *Pseudomonas aeruginosa* biofilms, but the underlying mechanism has not been explored (31).

The interactions between drugs were assessed using the highest-single-agent model (32), which presupposes that there are an active and an inactive drug in each combination, which is expected when an antibiotic and an antifungal agent are mixed. This model establishes additivity when the effect of the combination is not different from that of the most active drug alone and synergy (increased effect) when the effect of the combination is higher than that of the most active drug alone.

In brief, we showed that the drugs had limited activity when used alone against single-, dual-, or three-species biofilms and an additive effect when they were used in combination against single- or dual-species biofilms but increased (synergistic) effects, especially when caspofungin was combined with meropenem, to reduce the biomass of three-species biofilms.

RESULTS

Mixed-species biofilm models. A three-species biofilm model in 96-wells polystyrene plates including *S. aureus*, *E. coli* and *C. albicans* was previously set up (20). The

same protocol was used to grow the corresponding bacterium-fungus dual-species biofilms and single-species biofilms. The study of the evolution of the culturable cells and biomass over time for all models showed no significant difference between 48 and 72 h (Fig. S2), i.e., the time interval during which biofilms were incubated with the antimicrobials. Thus, any difference observed during this time frame is due to the activity of the antimicrobials.

Single-drug activity against culturable cells in planktonic cultures and biofilms.

The MICs of moxifloxacin and meropenem were 0.06 mg/L and 0.03 mg/L, respectively, against both bacteria but > 256 mg/L against *C. albicans*. The MIC of caspofungin was low against *C. albicans* (0.125 mg/L) but high against bacteria (64 and 32 mg/L against *S. aureus* and *E. coli*, respectively). The concentration-response curves for the activity of these antimicrobials against planktonic cultures and biofilms and the pharmacodynamic parameters maximal effect (E_{\max}), $C_{-1\log}$ and $C_{-90\%}$ are presented in Fig. 1 and Table 1. Drug activity was expressed as the change from the initial value measured at the time of drug addition (48-h precultured biofilms or initial inoculum for planktonic cultures). This reference time point was selected to compare activity in biofilms and planktonic cultures because biofilms remained stable during the incubation (Fig. S2) while planktonic cultures were growing. E_{\max} corresponds to the horizontal asymptote for the reduction in culturable cells or biomass from this reference time point, extrapolated for an infinitely large concentration of the drug. $C_{-1\log}$ and $C_{-90\%}$ correspond to the concentration of the drug required to reduce 90% of culturable cells (thus 1 log₁₀ CFU/well) or of biomass, respectively. Thus, they are measures of the relative potency of the drug.

Moxifloxacin (Fig. 1A to C) caused a significantly smaller reduction of culturable cells against both bacterial species in biofilms than in planktonic cultures and had no effect against *C. albicans*. It was more effective (more negative E_{\max}) against *S. aureus* in the single-species biofilm than in the *S. aureus*-*C. albicans* or three-species biofilms and against *E. coli* in single-species or *E. coli*-*C. albicans* biofilms than in the three-species biofilm. $C_{-1\log}$ values were close to those measured in planktonic cultures in all biofilms and for both species, except for *S. aureus* in the three-species biofilm, against which moxifloxacin was less potent (higher $C_{-1\log}$).

Meropenem (Fig. 1D to F) showed a reduced efficacy against *S. aureus* (though to a lesser extent against the *S. aureus*-*C. albicans* biofilm) and to a lower extent against *E. coli* (significant difference for single-species biofilm only) compared to the planktonic cultures. $C_{-1\log}$ values against bacteria were similar against planktonic cultures and all biofilms with the noticeable exception of the single-species biofilm of *E. coli*, against which meropenem was less potent. In other words, meropenem was more potent against *E. coli* in biofilms in which *C. albicans* was present, associated with *S. aureus* or not. No activity against *C. albicans* was observed.

Caspofungin (Fig. 1G to I) was active against planktonic *C. albicans* at low concentrations, with a $C_{-1\log}$ 10 times lower than the MIC and an E_{\max} of -2.3 log₁₀ CFU/well. Against bacteria, it started reducing the inoculum only at large concentrations. In biofilms, caspofungin did not show any effect against culturable *E. coli* cells and only little effect at high concentrations against *S. aureus*. Surprisingly, high concentrations were also needed to reduce *C. albicans* culturable cells in single-species and *S. aureus*-*C. albicans* biofilms, with $C_{-1\log}$ around 12 mg/L. The E_{\max} was not reached in most biofilms at the highest concentration tested.

Single-drug activity against biomass in biofilms. The concentration-response curves for the activity of these antimicrobials against biomass in biofilms and the corresponding pharmacodynamic parameters E_{\max} and $C_{-90\%}$ are presented in Fig. 2 and Table 1.

Moxifloxacin reduced biofilm biomass during the 24 h of incubation only in single-species biofilms of *S. aureus* or *E. coli*, but the E_{\max} was not reached at the highest concentration tested (Fig. 2A). The biomass of dual-species and three-species biofilms slightly increased after exposure to moxifloxacin (Fig. 2B). Meropenem reduced the biomass of bacterial single-species biofilms only, to 75 and 34% of the control value in

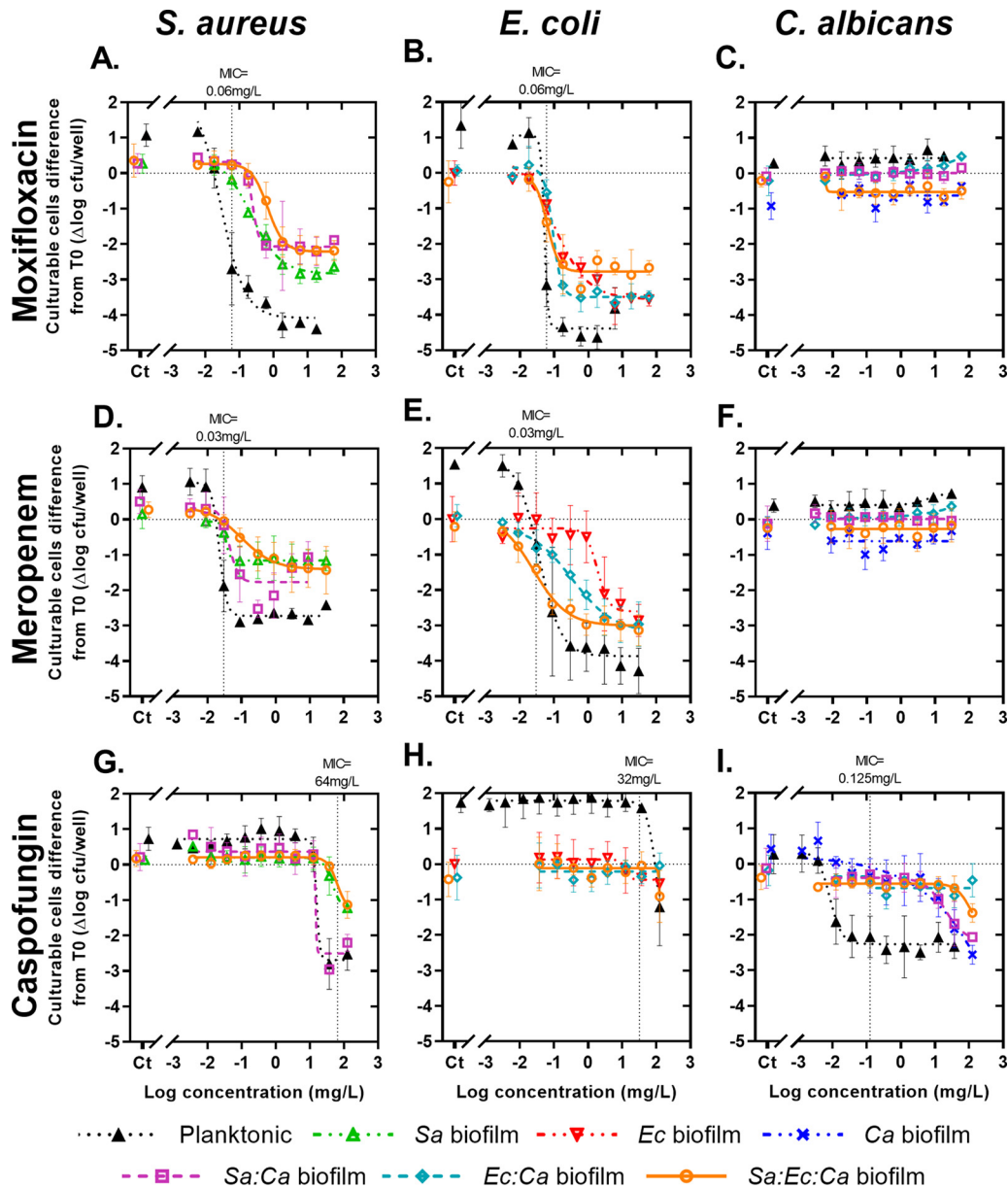


FIG 1 Activity of antimicrobials against culturable cells in planktonic cultures and biofilms after 24 h of incubation over a broad range of concentrations. Each row corresponds to one antimicrobial (moxifloxacin [A to C], meropenem [D to F], or caspofungin [G to I]); each column corresponds to one microorganism in all models, with the symbols explained at the bottom. The data are expressed as the difference between culturable cells at time zero (48-h biofilms or initial inoculum for planktonic bacteria) and 24 h treatment (72-h biofilms or 24 h of incubation for planktonic bacteria). $n = 3$ to 6. The horizontal dotted line shows the initial value of culturable cells; the vertical dotted line shows the MIC of each antimicrobial against the studied species. *Sa*, *S. aureus*; *Ec*, *E. coli*; *Ca*, *C. albicans*.

S. aureus and *E. coli* biofilms, respectively (Fig. 2C and D). Caspofungin caused significant reductions of biomass against dual-species, *E. coli*, and *C. albicans* biofilms, with the *S. aureus*–*C. albicans* biofilm being the most affected (Fig. 2E and F).

Activity of the moxifloxacin-caspofungin combination. A combination of moxifloxacin and caspofungin was then tested. Concentrations were adjusted to 1, 10, and 100 times their MICs against bacteria and *C. albicans*, respectively. These concentrations were selected to cover the range of concentrations over which moxifloxacin displayed a concentration-dependent effect when used alone as well as a range of clinically relevant concentrations (human maximum concentrations [C_{max}], 4 mg/L for

TABLE 1 Pharmacodynamic parameters describing the activity of moxifloxacin, meropenem and caspofungin on culturable cells and biomass after 24 h of incubation with planktonic or biofilm cultures^a

Test	Microorganism	Model ^b	E_{max} (log CFU/well or % AU) ^c			$C_{-10\log}$ or $C_{-90\%}$ (mg/L) ^d		
			Moxifloxacin	Meropenem	Caspofungin	Moxifloxacin	Meropenem	Caspofungin
Culturable cells	<i>S. aureus</i>	Planktonic	-4.1 ± 0.4 a, A	-2.8 ± 0.2 a, B	-2.7 ± 0.5 a, B	0.03 ± 0.01 d, D	0.02 ± 0.01 d, D	14.6 ± 13.1 d, D
		Sa biofilm	-2.8 ± 0.2 b, A	-1.1 ± 0.2 b, B	-1.3 ± 0.9*	0.19 ± 0.05 d, D	0.04 ± 0.04 d, D	71 ± 34.1 e, E
		Sa-Ca biofilm	-2.1 ± 0.2 c, A	-1.8 ± 0.4 c, A	-2.2 ± 0.4 a, A	0.25 ± 0.14 d, D	0.05 ± 0.03 d, D	31 ± 17.2 d, E
	<i>E. coli</i>	Sa-Ec-Ca biofilm	-2.2 ± 0.2 c, A	-1.2 ± 0.3 b, B	-1.3 ± 0.2*	0.68 ± 0.23 e, D	0.42 ± 0.85 d, D	100 ± 19.7 f, E
		Planktonic	-4.5 ± 0.2 a, A	-3.9 ± 0.5 a, A	-1.2 ± 1.4*	0.05 ± 0.04 d, D	0.03 ± 0.01 d, D	120.6 ± ND
		Ec biofilm	-3.4 ± 0.3 b, A	-2.8 ± 0.7 b, A	0 ± 0.2*	0.05 ± 0.02 d, D	1.37 ± 0.81 e, E	>125
<i>C. albicans</i>	Ec-Ca biofilm	-3.5 ± 0.2 b, A	-3.2 ± 0.8 ab, A	-0.4 ± 0.2*	0.07 ± 0.01 d, D	0.08 ± 0.07 d, D	>125	
	Sa-Ec-Ca biofilm	-2.8 ± 0.2 c, A	-3 ± 0.2 ab, A	-0.9 ± 0.7*	0.05 ± 0.02 d, D	0.01 ± 0.01 d, D	>125	
	Planktonic	0.5 ± 0.1*	0.5 ± 0.1*	-2.3 ± 0.2 a	>60	>30	0.01 ± 0 d	
	Ca biofilm	-0.6 ± 0.1*	-0.6 ± 0.1*	-2.5 ± 0.3*	>60	>30	12.9 ± 4.6 e	
	Sa-Ca biofilm	0 ± 0.1*	0 ± 0*	-2.2 ± 0.9 a	>60	>30	12.2 ± 8 e	
	Ec-Ca biofilm	0.1 ± 0.1*	0.3 ± 0*	-0.6 ± 0.4*	>60	>30	>125	
Biomass	<i>S. aureus</i>	Sa-Ec-Ca biofilm	-0.5 ± 0.1*	-0.5 ± 0.2*	-1.4 ± 0.3*	>60	>30	73.5 ± 20.5 f
		Sa biofilm	54.4 ± 20.6*	77.6 ± 17.6 a	115.5 ± 12*	>60	>30	>125
		Ec biofilm	64.7 ± 8.2*	33.5 ± 6.5*	69.7 ± 32 a	>60	>30	>125
	<i>E. coli</i>	Ca biofilm	112.3 ± 13 ab, A	112.8 ± 27.6 b, A	81.9 ± 4.8 a, B	>60	>30	>125
		Sa-Ca biofilm	127 ± 17*	91 ± 8.7 a	49 ± 5.7*	>60	>30	>125
		Ec-Ca biofilm	139 ± 12.7 a, A	133.2 ± 10.6 b, A	81 ± 1.4 a, B	>60	>30	>125
Sa-Ec-Ca biofilm	106.7 ± 8.4 b, A	87.2 ± 7.8 a, A	85 ± 16.5 a, A	>60	>30	>125		

^aData are based on concentration-response curves shown in Fig. 1 and 2. Statistical analysis for each microorganism and test was done with two-way ANOVA and Tukey posttest. Significant differences ($P < 0.05$) between models for the same drug are highlighted by different lowercase letters in the same column; those between different drugs for the same model are indicated by different uppercase letters in the same row. *, effect at 60, 30 or 125 mg/L of moxifloxacin, meropenem, or caspofungin, respectively (highest concentrations tested). Not considered for the statistical comparisons of E_{max} .

^bSa, *S. aureus*; Ca, *C. albicans*; Ec, *E. coli*.

^cMaximal reduction for culturable cells (log CFU/well) or biomass (% AU), extrapolated from the concentration-response curve for an infinitely large concentration.

^dConcentration needed to reduce of 90% the culturable cells ($-1 \log$) or of 90% the biomass ($C_{-90\%}$), calculated from the concentration-response curve. ND, not determined.

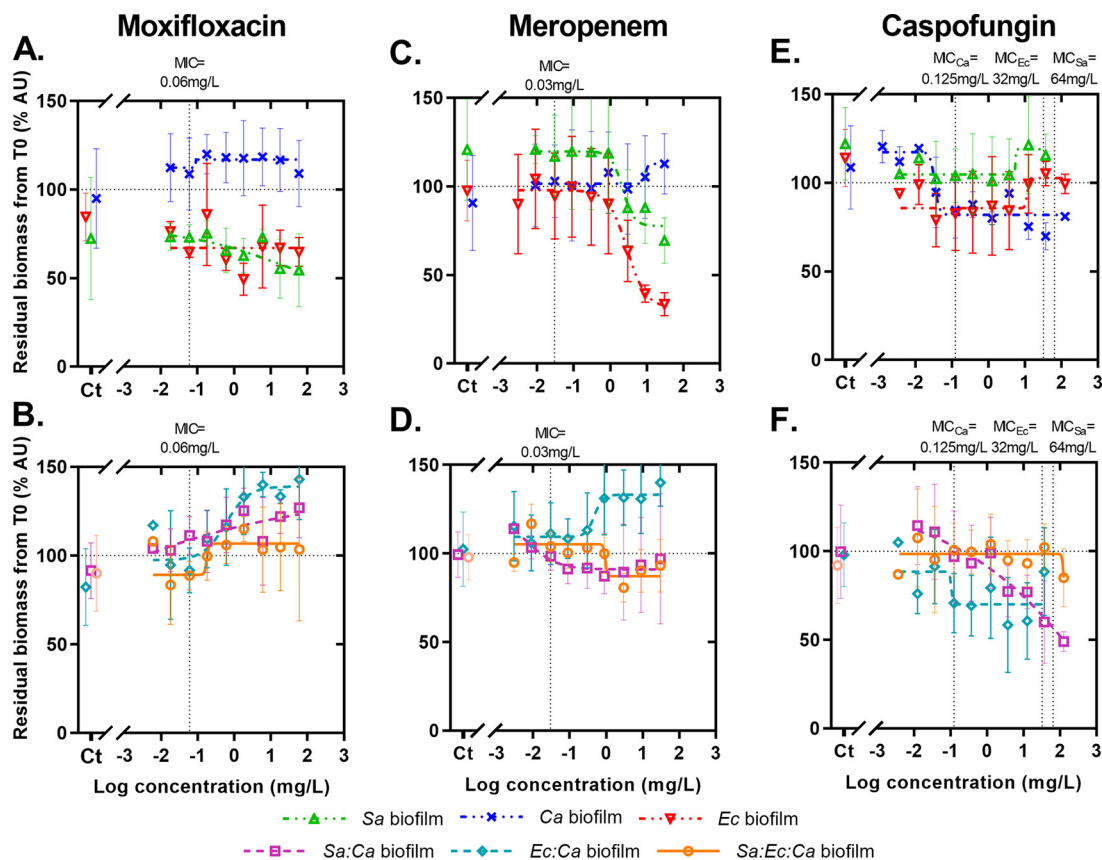


FIG 2 Activity of antimicrobials against biomass of biofilms after 24 h of incubation over a broad range of concentrations. Each column corresponds to one antimicrobial (moxifloxacin [A and B], meropenem [C and D], and caspofungin [E and F]); the top row shows results for single-species biofilms, and the bottom row shows to dual- or three-species biofilms, with the symbols defined at the bottom. The data are expressed as the difference between culturable cells at time zero (48-h biofilms) and 24 h treatment (72-h biofilms). $n = 3$ to 6. The horizontal dotted line shows the biomass value at time zero (100%); the vertical dotted line shows the MIC of each antimicrobial against the studied species. *Sa*, *S. aureus*; *Ec*, *E. coli*; *Ca*, *C. albicans*.

moxifloxacin [70 times the MIC against bacteria] [33] and 13.8 mg/L [free drug; highly protein-bound drug] for caspofungin [110 times the MIC against *C. albicans*] [34]).

Figure S3 and Fig. 3 show the results obtained for culturable cells of each microorganism in planktonic cultures and each biofilm, respectively. In planktonic cultures, an additive effect was generally observed, with reductions in culturable cells close to the effect of the active single agent in most cases. However, a decreased effect (antagonism) was noticed at high concentrations of caspofungin against *S. aureus* or at low concentrations of moxifloxacin against *E. coli* (Fig. S3A and B), or an increased effect (synergy) at a high concentration of caspofungin and low concentration of moxifloxacin against *C. albicans* (Fig. S3C).

An additive effect was observed in single-species, *S. aureus*–*C. albicans*, and three-species biofilms for all organisms (Fig. 3A to E and H to J). A decreased effect was noticed regarding *E. coli*, which reached significance in the *E. coli*–*C. albicans* biofilm but not in the *E. coli* single-species or the three-species biofilms (Fig. 3B and F). No interaction was observed regarding *C. albicans* in the same biofilm exposed to drug combinations (Fig. 3G).

Considering then the biomass of each type of biofilm (Fig. 4), an additive effect against single-species or dual-species biofilms was observed (Fig. 4A to E), but a strong synergy (increased effect) was noticed against the three-species biofilm when at least one of the two antimicrobials was present at the highest concentration tested, decreasing the biomass by 20% to 30% (Fig. 4F).

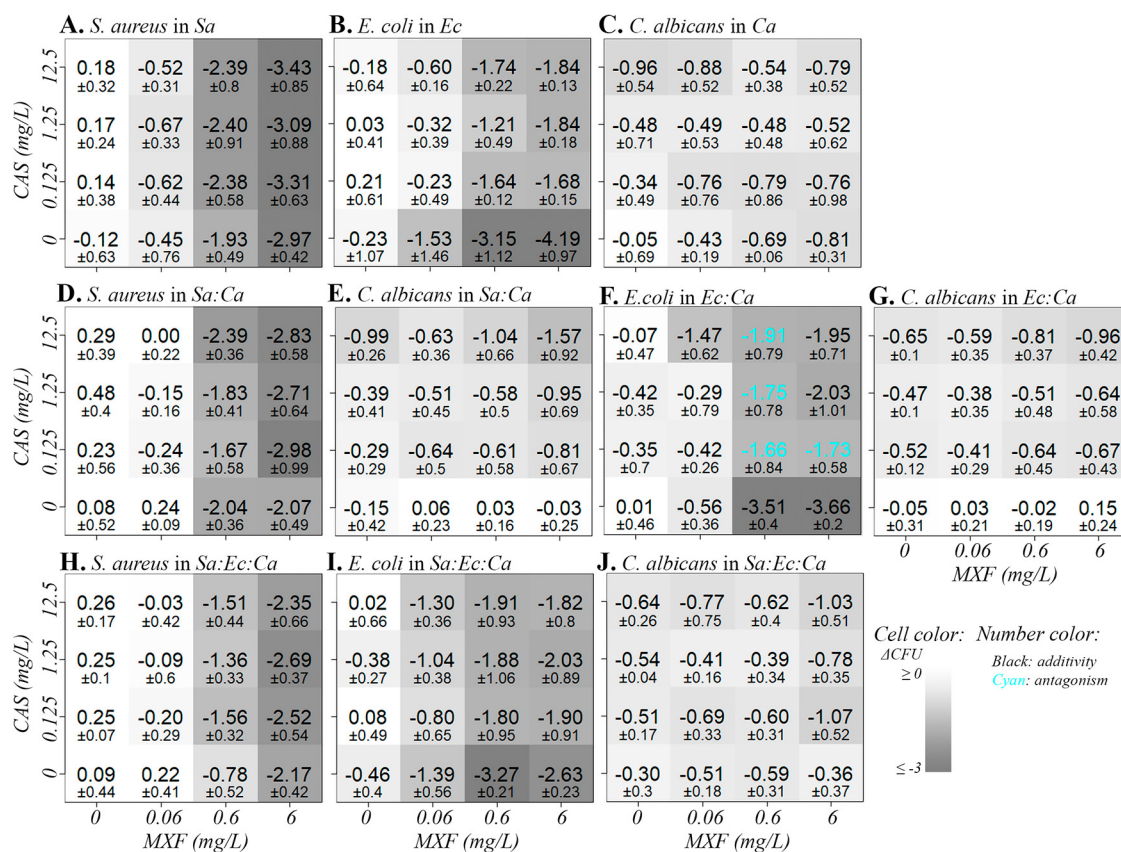


FIG 3 Effect (average and standard deviation [SD]) against the culturable cells in biofilms ($\Delta\log_{10}$ CFU/well) of the combination of moxifloxacin and caspofungin for 24 h and its synergy/antagonism (increased/decreased effect). Each drug was used at three selected concentrations; data for single drugs at the concentrations used in combination are repeated for clarity. The effect is shown in gray scale (darker shade means more effect). Black numbers show additivity (no interaction); cyan numbers show a decreased effect (antagonism; $P < 0.05$). Moxifloxacin (MXF) and caspofungin (CAS) concentrations are in milligrams per liter.

Activity of the meropenem-caspofungin combination. A combination of meropenem and caspofungin was also tested following a similar design, except that the concentrations selected for meropenem were 10 times higher than those of moxifloxacin (10, 100, and 1,000 times the MIC) to fully cover the zone of concentration dependency of its activity, to reach the plateau of maximal efficacy in all biofilms, and to better cover the range of clinically relevant concentrations for this drug (human C_{\max} 40 mg/L for a dose of 2 g [670 times the MIC against bacteria] [35]).

The combination was examined against culturable cells in planktonic cultures and biofilms (Fig. S4 and Fig. 5). In planktonic cultures, additive effects were observed in most of the cases, and thus, there was no gain or loss from the effect of the active single agent. Nevertheless, a synergy at a high concentration of caspofungin against *C. albicans* (Fig. S4C) and a decreased activity at a high concentration of caspofungin and low concentration of meropenem against *E. coli* (Fig. S4B) were observed.

In the single-species biofilms, meropenem and caspofungin showed significant interactions but with different patterns. Caspofungin increased the effect of meropenem at 0.3 mg/L against *S. aureus* (Fig. 5A) and at any concentration against *E. coli* (Fig. 5B). Conversely, meropenem increased the effect of caspofungin at 0.125 mg/L against *C. albicans* (Fig. 5C). For the dual-species biofilms, an additive effect was observed against *S. aureus* (Fig. 5D), but caspofungin increased the effect of meropenem at 0.3 mg/L against *E. coli* (Fig. 5F). Again, meropenem slightly increased the effect of caspofungin against *C. albicans* in both dual-species biofilms, but the synergy reached significance only in the *S. aureus*–*C. albicans* biofilm and for the lowest concentrations of caspofungin (Fig. 5E, G).

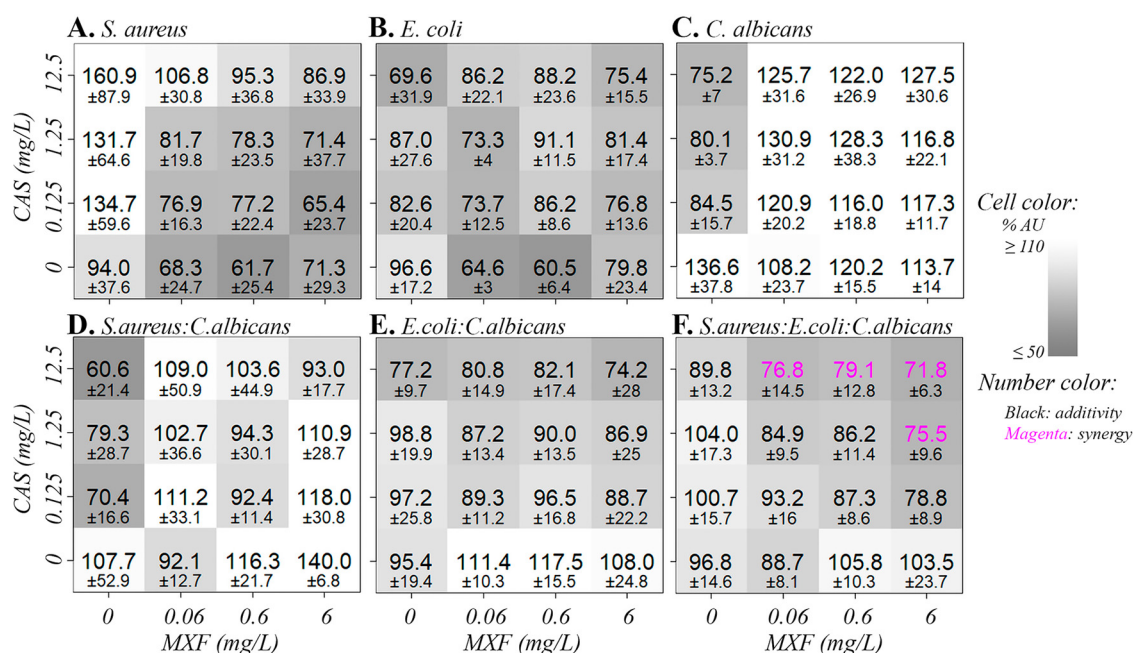


FIG 4 Effect (average and SD) against the biomass of the biofilms (% absorbance units [AU]/well) of the combination of moxifloxacin and caspofungin for 24 h, and its synergy/antagonism (increased/decreased effect). Each drug was used at three selected concentrations; data for single drugs at the concentrations used in combination are repeated for clarity. The effect is shown in gray scale (darker shade means more effect). Black numbers show additivity (no interaction); magenta numbers show increased effect (synergy; $P < 0.05$). Moxifloxacin (MXF) and caspofungin (CAS) concentrations are in milligrams per liter.

In the three-species biofilm, an additive effect was observed for *S. aureus* (Fig. 5H). Interestingly, the patterns against *E. coli* and *C. albicans* were opposite to each other (Fig. 5I and J): caspofungin reduced the effect of meropenem against *E. coli*, while meropenem markedly increased the effect of caspofungin against *C. albicans*.

Against biomass (Fig. 6), an increase in activity was observed for the combination between meropenem and caspofungin against the single-species and the three-species biofilms (Fig. 6A to C and F). The reduction in biomass in the three-species biofilm reached around 40%. However, only an additive effect was observed against the dual-species biofilms (Fig. 6D and E).

Confocal microscopy with live/dead staining. Figure 7 shows images from confocal microscopy of biofilms grown on Ti coupons and exposed to a combination of moxifloxacin-caspofungin or meropenem-caspofungin at the highest concentrations tested previously (i.e., 6/12.5 and 30/12.5 mg/L, respectively), for 24 h. The pictures show qualitative trends similar to those observed in biofilms grown in microtiter plates.

For single-species biofilms, the highest proportion of dead bacteria was observed in the *S. aureus* biofilm after incubation with moxifloxacin-caspofungin. A similarly high reduction of approximately 3 log₁₀ CFU was measured in microtiter plates for *E. coli* biofilms exposed to meropenem-caspofungin, but the predominant effect seen in the confocal image was the marked reduction in biomass, also described in quantitative experiments (28% of residual biomass). The images of *S. aureus* biofilm exposed to meropenem-caspofungin and *E. coli* biofilms exposed to moxifloxacin-caspofungin looked similar, in accordance with our quantitative results. A slightly higher proportion of dead cells were visible in the treated *C. albicans* biofilm than in the corresponding control.

For the dual-species biofilms, dead cells were more visible in biofilms incubated with the combination moxifloxacin-caspofungin, while the reduction in biomass was more visible after incubation with the meropenem-caspofungin combination, as in our quantitative experiments.

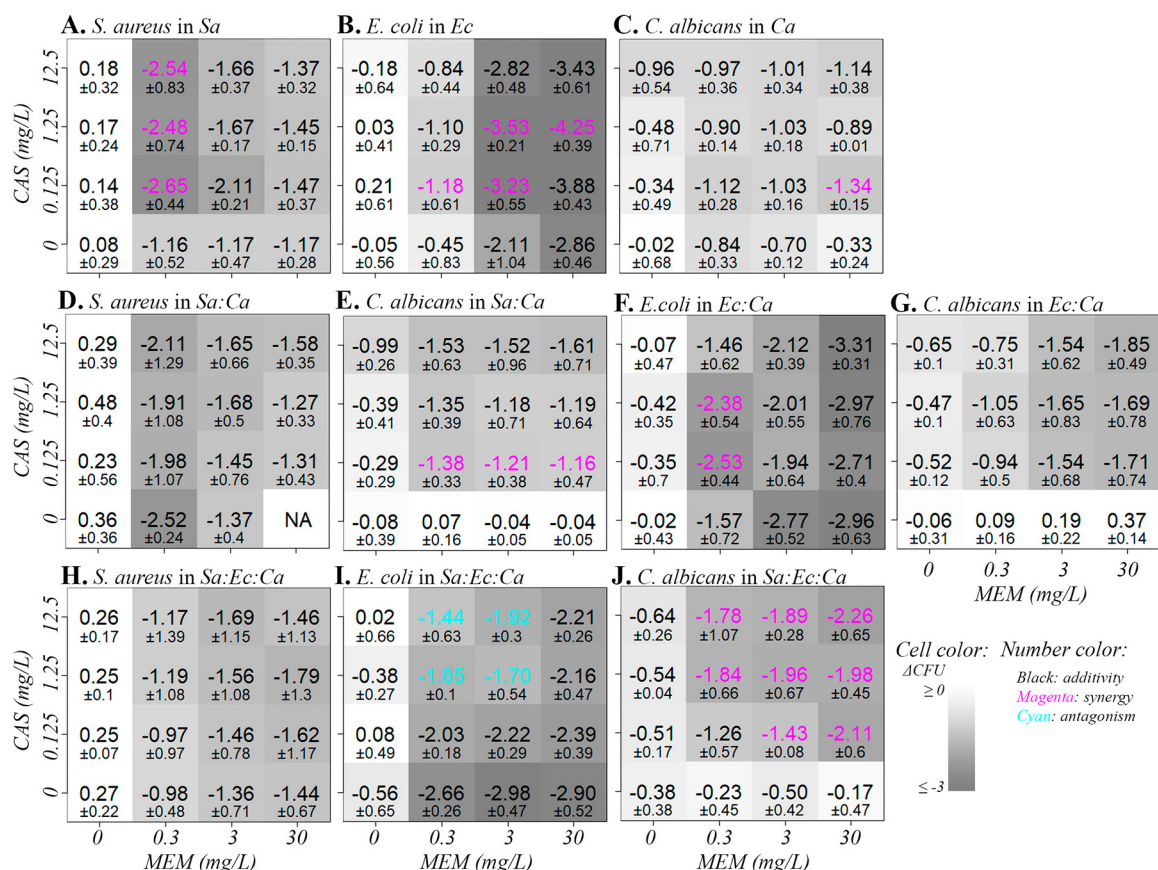


FIG 5 Effect (average and SD) against the culturable cells in biofilms ($\Delta \log_{10}$ CFU/well) after the combination of meropenem and caspofungin for 24 h and its synergy/antagonism (increased/decreased effect). Each drug was used at three selected concentrations; data for single drugs at the concentrations used in combination are repeated for clarity. The effect is shown in gray shade (darker shade means more effect). Black numbers show additivity (no interaction); magenta numbers show increased effect (synergy; $P < 0.05$); cyan numbers show decreased effect (antagonism; $P < 0.05$). Meropenem (MEM) and caspofungin (CAS) concentrations are in milligrams per liter.

For the three-species biofilm, both combinations markedly reduced the biomass, and a substantial proportion of *C. albicans* cells were dead after incubation with meropenem-caspofungin, as also observed in 96-well plates.

Relative abundance of polysaccharides. The abundance of polysaccharides was determined after incubation with moxifloxacin at 6 mg/L, meropenem at 30 mg/L, caspofungin at 12.5 mg/L and moxifloxacin-caspofungin or meropenem-caspofungin at the same concentrations. The relative abundance in each sample (i.e., the quantity of polysaccharides normalized to the total biomass of the corresponding biofilm assessed by the absorbance of crystal violet) was compared to the value measured in the corresponding control biofilm (incubation without antimicrobials) (Fig. 8; values of absolute amounts of polysaccharides and optical density [OD] of crystal violet are presented in Fig. S5).

A lower relative abundance of polysaccharides was observed in all biofilms incubated with each of the combinations of antimicrobials (moxifloxacin-caspofungin or meropenem-caspofungin) compared to control biofilms, except for the *E. coli* biofilm (Fig. 8B). For drugs used alone, caspofungin was the only one to reduce the polysaccharide relative abundance in all biofilms (except *E. coli* biofilms, for which an increase was observed), although this effect did not reach statistical significance.

DISCUSSION

While some studies have explored the activity of antibiotics and antifungals against both single- and dual-species biofilms (17, 30, 36), only a few of them have included

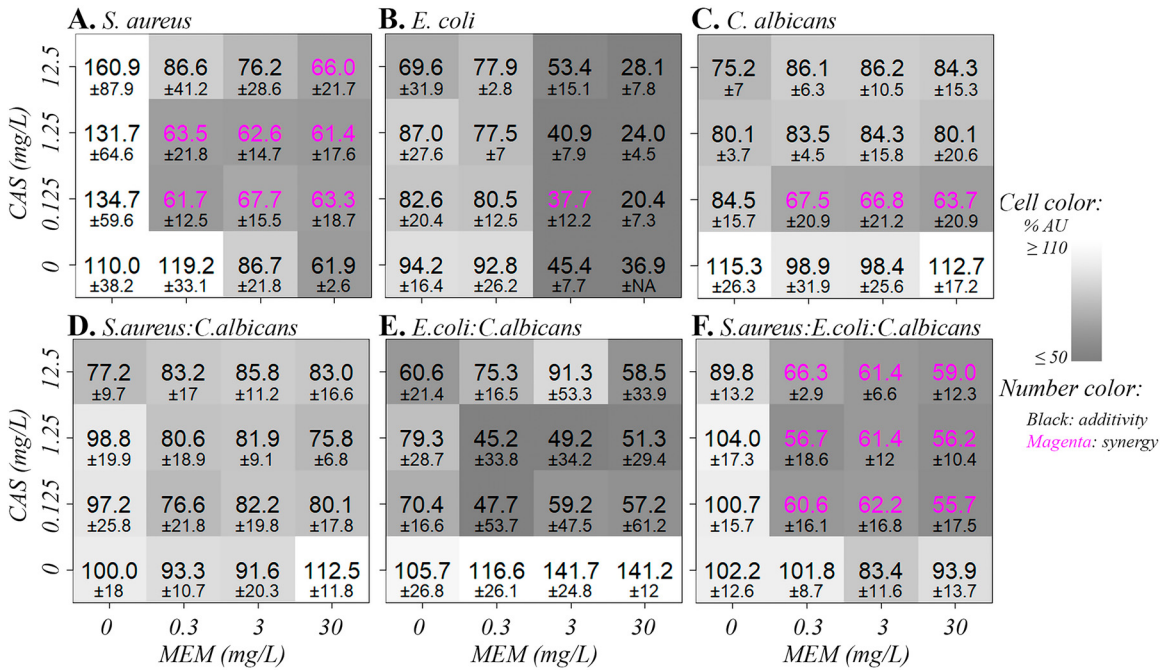


FIG 6 Effect (average and SD) against the biomass of the biofilms (% AU/well) after the combination of meropenem and caspofungin for 24 h and its synergy/antagonism (increased/decreased effect). Each drug was used at three selected concentrations; data for single drugs at the concentrations used in combination are repeated for clarity. The effect is shown in gray scale (darker shade means more effect). Black numbers show additivity (no interaction); magenta numbers show increased effect (synergy; $P < 0.05$). Meropenem (MEM) and caspofungin (CAS) concentrations are in milligrams per liter.

the selection of antimicrobials explored in this work (37, 38) or tested them against interkingdom biofilms (16, 18, 19, 39). Moreover, this study is, to the best of our knowledge, the first one to assess on a pharmacodynamic basis the nature of the drug interactions against the pathogens used in the three-species biofilm model.

Considering first the activity of single agents against single-species biofilms, we globally observed that antibiotics are less effective, but not necessarily less potent, against biofilms than planktonic bacteria, while caspofungin was less potent in *Candida* biofilms and showed only minimal efficacy except at high concentrations. Although few studies ran full concentration-response curves allowing for a direct comparison with our work, some previous publications also showed that moxifloxacin was more effective than meropenem against *S. aureus* biofilms (29, 40, 41), that the fluoroquinolone levofloxacin was more potent and effective than meropenem against *E. coli* biofilms (42), or that caspofungin potency was reduced in biofilms (43). The lack of effect of caspofungin against single-species or *E. coli*-*C. albicans* biofilms was reported previously (16, 19). Despite this global loss of efficacy, it is worth mentioning that reductions superior to $2.5 \log_{10}$ CFU were observed against *E. coli* biofilm for both antibiotics or moxifloxacin against *S. aureus* when they were used at concentrations close to their respective human C_{max} (around 4 and 40 mg/L for doses of 400 mg and 2 g, respectively [33, 35]). Nevertheless, there was always a high proportion of bacterial persistence, ranging from 10^3 to 10^5 CFU/well in all biofilms.

Regarding the activity of single agents against mixed-species biofilms, moxifloxacin was less effective against *S. aureus* in the three- and dual-species biofilm than against the single-species biofilm. It was also less effective against *E. coli* in the three-species biofilm than in the single-species or dual-species biofilm. This could be ascribed to a protective role of the *C. albicans* polysaccharidic matrix (16, 17), but the reason why this does not apply to meropenem remains to be established. This behavior contrasts with that of meropenem, for which the major difference observed among biofilm models concerns its potency. It was markedly reduced against *E. coli* in single-species

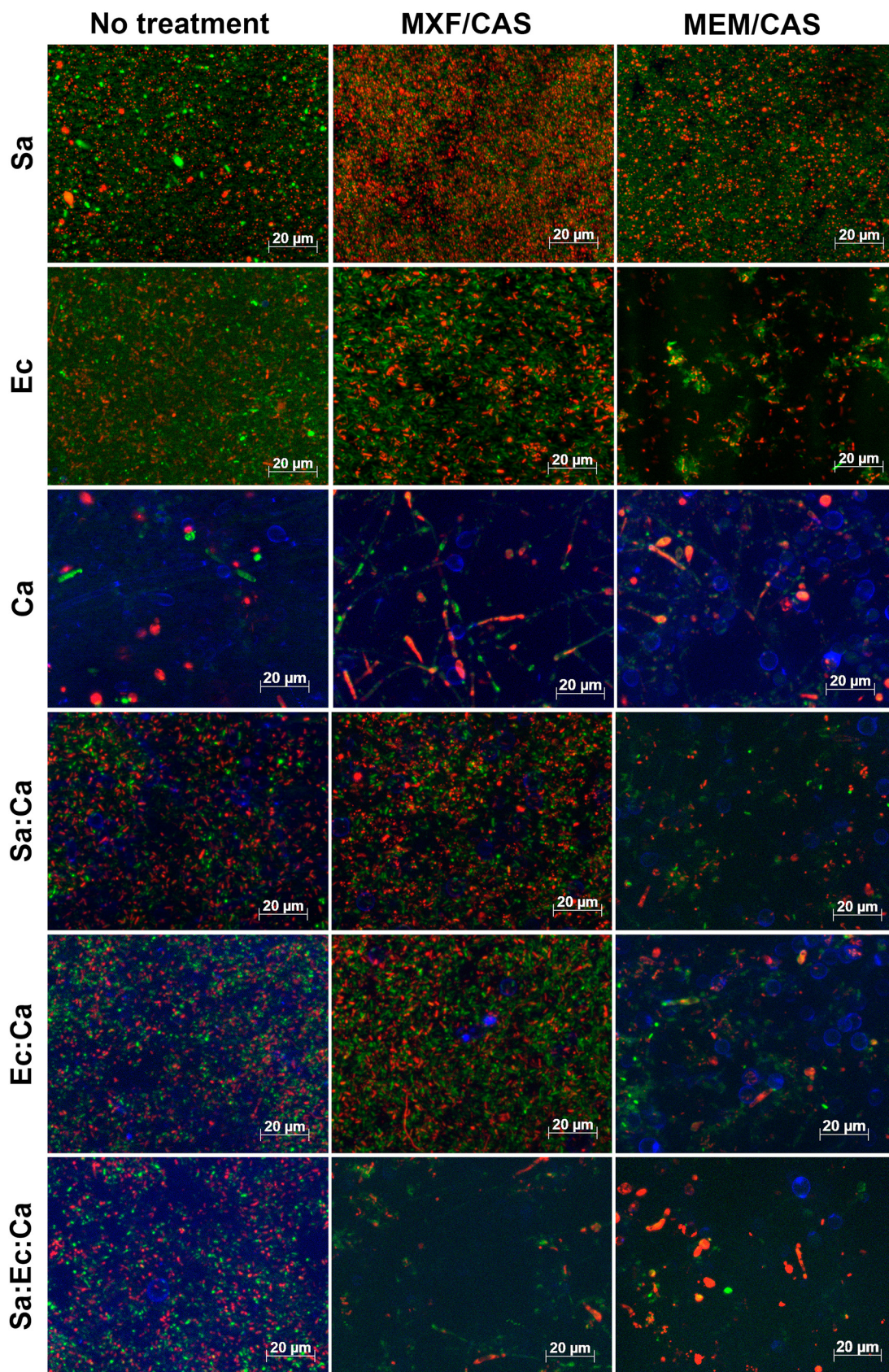


FIG 7 Confocal images of biofilms after live/dead staining. Biofilms grown on Ti alloy coupons were incubated for 24 h with combinations of moxifloxacin-caspofungin (6 and 12.5 mg/L) or meropenem-caspofungin (30 and 12.5 mg/L). Green, intact cells (live); red, disrupted cells (dead); blue, *C. albicans* yeasts and hyphae. Sa, *S. aureus*; Ec, *E. coli*; Ca, *C. albicans*.

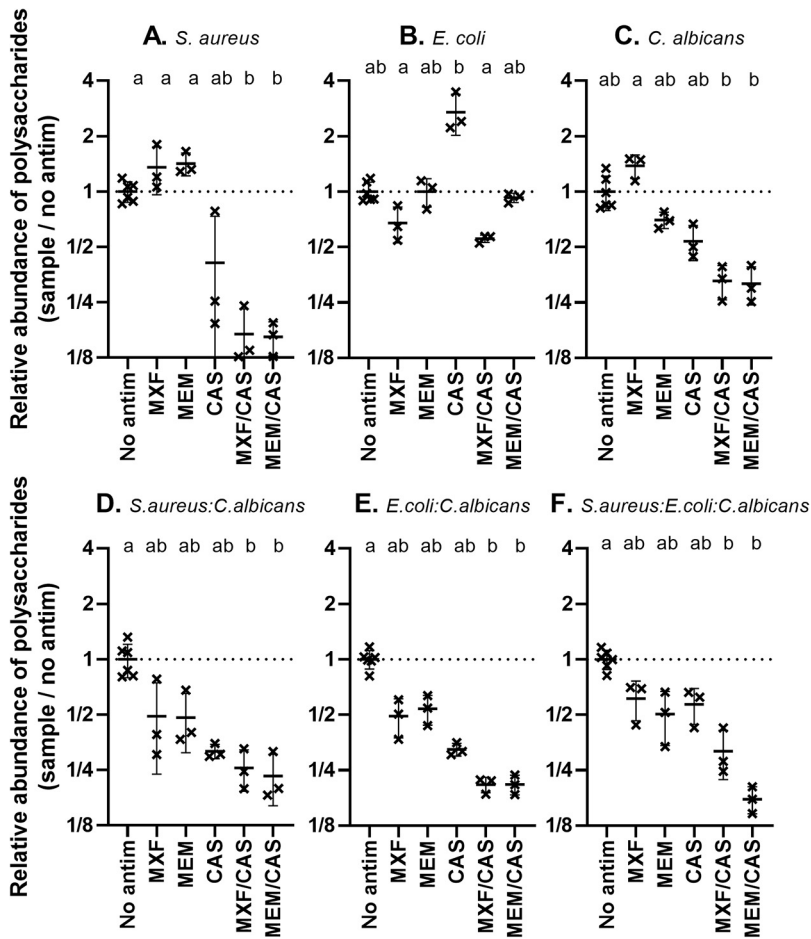


FIG 8 Relative abundance of polysaccharides after incubation with antimicrobials, expressed as the ratio to the value measured in the corresponding control (no antimicrobial added). The abundance itself was calculated as the ratio between the quantity of polysaccharides, estimated with the periodic acid-Schiff method, and the total biomass, estimated with the crystal violet assay. MXF, moxifloxacin (6 mg/L); MEM, meropenem (30 mg/L); CAS, caspofungin (12.5 mg/L). $n = 3$ to 6. Different letters denote significant differences ($P < 0.05$; one-way nonparametric analysis of variance [ANOVA], Tukey posttest).

biofilms versus planktonic cultures or mixed species biofilms, in spite of the fact that *E. coli* activates stress responses in interkingdom biofilms (20).

Both moxifloxacin and meropenem reduced biomass in the bacterial single-species biofilms but not in *C. albicans* biofilm, which was expected. The fact that moxifloxacin increased the biomass in both dual-species biofilms and meropenem in the *E. coli*-*C. albicans* biofilm might be explained by the killing of bacterial cells by the antibiotics, which reduces competition for *C. albicans* to produce matrix. The poor effect of meropenem against *S. aureus* may explain why a similar trend was not observed in the *S. aureus*-*C. albicans* biofilm incubated with this antibiotic. Caspofungin effects on biomass were essentially observed against *S. aureus*-*C. albicans* biofilms, probably related to its capacity to also reduce not only the production of polysaccharides but also the number of culturable cells of *S. aureus* and of *C. albicans* (at high concentrations). The latter contribute to biomass due to their large volume. Reactive oxygen species (ROS) production, bacterial killing, and decreased biofilm formation have been documented in methicillin-resistant *S. aureus* (MRSA) exposed to caspofungin, but only when very high concentrations were used in low-ionic-content solutions and not in RPMI medium (44).

Comparing the activity of single drugs and their combinations against planktonic cultures showed that the activity of caspofungin at high concentrations was potentiated by

moxifloxacin or meropenem, which is in agreement with previous works combining caspofungin with β -lactams *in vitro* or *in vivo* (45, 46). On the other hand, the decreased activity observed for specific combinations against *S. aureus* and, more often, against *E. coli* planktonic cultures have never been described and remained unexplained. Unexpected effects of caspofungin on bacterial metabolism have been described but only for *Enterococcus faecium*, in which caspofungin instead facilitates the activity of vancomycin (47).

In biofilms, additive effects were observed in most cases, ensuring a reduction of all microorganisms in the biofilms as well as of the global biomass. However, salient increases in activity were observed in the biomasses of three-species biofilms exposed to both types of combinations. Additional synergies were noticed for specific concentration ratios of combinations with meropenem; they concern bacterial counts in single- or dual-species biofilms and fungal counts in three-species biofilms, as well as biomass of single-species biofilms. A reason why synergy is more frequently seen when the combined antibiotic is meropenem could reside in its own lower activity compared to moxifloxacin. Previous studies demonstrated the important activity of antibiotic-echinocandin combinations in *S. aureus*-*C. albicans* biofilms *in vitro* or *in vivo*, but the analyses were not performed in such a way as to be able to establish whether the interaction was pharmacologically synergistic (39). It is also remarkable that increases in activity are primarily seen with biomass and related to a reduction in the relative abundance of polysaccharides. This may at least partially result from the previously described effects of echinocandins on bacterial biofilms, i.e., impairment of PNAG synthesis in *S. aureus* biofilms (29) or a reduction in biofilm production for another Gram-negative species, *Pseudomonas aeruginosa* (31). Indeed, PNAG plays multiple other roles in both fungi and bacteria, which could be perturbed as well by the echinocandin, including hypha formation, production of fimbriae and curli fibers in *E. coli*, regulation of metabolic pathways, and building of peptidoglycan (48). This mechanism does not seem to apply to *E. coli* in our case, since PNAG relative abundance in *E. coli* biofilm was not reduced by caspofungin. Although present in *E. coli* biofilms (49), PNAG is considered a minor constituent of the matrix, which is mainly made up of proteinaceous curli fibers and flagella and the polysaccharide cellulose (50). Incidentally, a significant reduction in activity regarding culturable *E. coli* cells was noticed with moxifloxacin in single- and dual-species biofilms and with meropenem in three-species biofilms at specific concentrations, in the line with our observations in planktonic cultures.

The model used in this study has several limitations. First, it is an endpoint model under optimal conditions that does not consider the dynamics of the biofilm over time. Second, the polystyrene surface or geometry of the wells used for growing biofilms is not clinically relevant and may influence the architecture of the biofilm or the nature of the produced matrix (51). The implementation of surfaces like Ti, steel, or silicone, not only for microscopy, might be useful, although it would be impractical and expensive for relatively high-throughput experiments. Third, we used reference strains, which may differ from clinical isolates in their capacity to form biofilms or in the nature of the matrix they produce (52–54). This was a necessary step to set up a new model, but expanding the experiments to clinical strains would allow us to confirm our findings in a broader context.

Nevertheless, our *in vitro* findings highlight the interest of combining caspofungin with antibiotics for the treatment of interkingdom biofilms, with moxifloxacin being preferable when targeting *S. aureus* and meropenem when targeting *E. coli*, at least for isolates demonstrating susceptibility to these drugs.

MATERIALS AND METHODS

Strains, growth conditions, and materials. We used the reference strains *S. aureus* ATCC 25923, *E. coli* ATCC 47076, and *C. albicans* ATCC 24433, commonly used as references in experiments dealing with the evaluation of antimicrobial agents against biofilms (for a few examples, see references 55–59). Their ability to form biofilms was controlled in comparison to clinical isolates in Fig. S6. They were maintained in Mueller-Hinton broth with 10% glycerol at -80°C . For all experiments, precultures were prepared from a frozen aliquot on tryptone soy agar (TSA; Becton Dickinson [BD], Franklin Lakes, NJ) and Sabouraud glucose agar (SGA; peptone [10 g/L], D -glucose [40 g/L], agar [15 g/L]), for the bacteria and *C. albicans*, respectively, and incubated overnight at 37°C . Aliquots were discarded after thawing.

Two media were used to culture the biofilms, both based on RPMI 1640 supplemented with L-glutamine (Sigma-Aldrich, St. Louis, MO) and filter sterilized: RGP is RPMI with phosphate buffer (KH_2PO_4 [50 mM], Na_2HPO_4 [74.1 mM]; pH 7.4) and 10 g/L of glucose, and RH is RPMI with 25 mM HEPES. Inocula were prepared in phosphate-buffered saline (PBS; NaCl [137 mM], KCl [2.7 mM], Na_2HPO_4 [8 mM], KH_2PO_4 [1.5 mM]). The following selective agar media were used for CFU counting: modified mannitol salt agar (MSA; peptone [5 g/L], NaCl [75 g/L], D-mannitol [10 g/L], agar [15 g/L], amphotericin B [5 mg/L]) for *S. aureus*; selective TSA (TVA; TSA with 5 mg/L vancomycin and 5 mg/L amphotericin B) for *E. coli*; selective SGA (S4; SGA with 15 g/L agar [pH 4.5]) for *C. albicans*. Antimicrobials were added when the temperature was below 60°C after autoclaving the media.

Moxifloxacin HCl (microbiological standard; potency 97%) was kindly provided by Bayer, Leverkusen, Germany. The other drugs were obtained as the corresponding branded products registered for human parenteral use in Belgium or as microbiological standards with the following potencies: meropenem, 100% (Hospira, Brussels, Belgium); vancomycin, 100% (Mylan, Hoeilaart, Belgium); caspofungin, 50% (as Candidas; MSD, Kenilworth, NJ); cyclosporine, 100%; and soluble amphotericin B, 45% (Sigma-Aldrich). The concentrations of excipients in the formulations of caspofungin and amphotericin B, notably acetic acid and deoxycholate acid, respectively, are below those described as harmful for microbial cultures (60, 61) under our experimental conditions. Stock solutions were prepared at 1 mg/ml in sterile Milli-Q water for moxifloxacin and meropenem and 2 mg/ml in dimethyl sulfoxide (DMSO) for caspofungin and cyclosporine, stored at -20°C , and used within 3 weeks. Amphotericin B and vancomycin were prepared in sterile Milli-Q water and used immediately.

MIC. The microdilution broth assay was performed as described in CLSI and EUCAST guidelines for bacteria and *C. albicans*, respectively, using RGP instead of standard medium (62, 63). For *C. albicans*, and to avoid a paradoxical growth (Fig. S7), 1 mg/L of cyclosporine was added to all concentrations of caspofungin (MIC of cyclosporine versus *S. aureus*, *E. coli*, or *C. albicans*, >32 mg/L).

Biofilm culture. Biofilms were cultured as described by Ruiz-Sorribas et al. (20). Briefly, biofilms were grown in polystyrene tissue culture plates (96 wells, F surface treated; VWR, Radnor, PA). The inoculum was adjusted to 1.5×10^7 CFU/ml *S. aureus* in RGP, 6×10^6 CFU/ml *E. coli* in RGP, or 2.5×10^6 CFU/ml *C. albicans* in RH, in order to obtain a stable biofilm (20). The plates were incubated 24 h at 37°C, and the medium was discarded by inversion to a beaker, for bacteria that were firmly attached to the bottom of the plates, or aspiration with a pipette, for *C. albicans*. In order to avoid any risk of cross-contamination among the different biofilm models, each plate contained a single type of biofilm. The absence of gross contamination from well to well or from the environment was also checked by including noninoculated control wells at the edges of each plate. For single-species biofilms, fresh RGP was added very gently to the wells. For dual- or three-species biofilms, RGP was inoculated with *S. aureus* and/or *E. coli* at the inocula listed above to precultured *C. albicans* 24-h biofilms. Plates were incubated for another 24 h at 37°C.

Alternatively, the same protocol was used to culture the biofilms on Ti alloy disc coupons (Ti-6Al-4V ELI; diameter, 12.7 mm; thickness, 3.8 mm; BioSurface Technologies, Bozeman, MT). Coupons were incubated with gentle agitation at 50 rpm. Coupons were reconditioned according to an adapted protocol from BioSurface Technologies (64). Briefly, used coupons were immersed in 0.1% (vol/vol) RBS soap and sonicated for at least 10 min, rinsed in running water, and sonicated repeatedly in water until no foam was produced, after which they were immersed in 2 M HCl for 2 h, rinsed with Milli-Q water, let dry at 60°C, and autoclaved.

Incubation of biofilms and planktonic cultures with antimicrobials. Precultured 48-h biofilms in 96-well plates were exposed to antimicrobials alone or in combination. Biofilms were washed once with PBS. Fresh RGP containing moxifloxacin, meropenem, caspofungin, or combinations of each of the two antibiotics with caspofungin was added. Cyclosporine (1 mg/L) was added when caspofungin was present (we checked that cyclosporine did not prevent the growth of the controls). Plates were incubated for 24 h at 37°C.

In parallel, the same drugs or combinations were tested against planktonic cells. In a 15-ml tube, 2 ml of RGP with moxifloxacin, meropenem, caspofungin, or combinations of each of the antibiotics with caspofungin was inoculated with either 7.5×10^6 CFU/ml *S. aureus*, 3×10^6 CFU/ml *E. coli*, or 1.25×10^6 CFU/ml *C. albicans*. Caspofungin solutions were always supplemented with 1 mg/liter of cyclosporine. Tubes were incubated 24 h at 37°C under gentle agitation at 130 rpm. Cells were washed with PBS by two successive centrifugations at $3,000 \times g$ (a force low enough to preserve cell viability [65]) well and resuspended in the initial volume in PBS. An appropriate dilution was performed, and 50 μL was transferred to TSA or SGA. Colonies were counted after overnight incubation.

Culturable cells from biofilms. After removal of the medium, biofilms were detached by mechanically scratching the surface with an inoculation loop and resuspending in 200 μL of PBS with vigorous pipetting. Quality controls were routinely performed to ensure appropriate detachment of the biofilms (Fig. S8). The resuspended biofilms were disaggregated by sonication (Q700 sonicator; QSonica, Newton, CT) at 60% amplitude for 30 s directly in the well. The suspension was recovered, and two wells were pooled and diluted appropriately. In the case of three- and dual-species biofilms, 50 μL of the same dilution series was transferred to the appropriate selective agar. In the case of bacterial or *C. albicans* single-species biofilms, the same volume was transferred to TSA or SGA, respectively. Agar plates were incubated at 37°C. Colonies on TSA or TVA were counted after overnight incubation. Colonies on SGA or S4 plates were counted after 24 h, and colonies on MSA were counted after 48 h. Data were expressed as the change in CFU from the initial inoculum (time zero, corresponding to 48 h of biofilm preculture or to 0 h for planktonic cultures).

Biomass assay. Total biomass was estimated with the protocol detailed by Ruiz-Sorribas et al. (20). Briefly, after removal of the medium, biofilms were dried at 60°C. A volume of 200 μL of crystal violet (Sigma-Aldrich) at 0.5% (vol/vol) (final concentration, 115 mg/L) in water was used to stain the dried biofilms for 10 min at room temperature. Nonbound crystal violet was rinsed in running water. Bound

crystal violet was resuspended in 200 μL of acetic acid 66% (vol/vol) (Merck, Darmstadt, Germany) in water for at least 1 h in darkness. Resuspended crystal violet was quantified by absorbance at 570 nm using a microplate reader (SpectraMax Gemini XS microplate spectrophotometer; Molecular Devices LLC, San José, CA). Data were expressed as the change in absorbance, using as a reference (100%) the value measured at time zero, corresponding to 48 h of biofilm preculture.

Relative abundance of polysaccharides. The abundance of polysaccharides was estimated as the ratio between the quantity of polysaccharides and total biomass. Polysaccharides were quantified using the periodic acid-Schiff assay with a protocol adapted from those of Randrianjatovo-Gbalou et al. and Kilcoyne et al. (66, 67). Briefly, biofilms were incubated with 25 μL of PBS and 175 μL 10 mM of *ortho*-periodic acid (Fisher Scientific, Waltham, MA) in acetic acid 5% (vol/vol) for 30 min at room temperature in darkness. One hundred microliters of Schiff reagent (Sigma-Aldrich) was added and incubated for another 60 min at room temperature in darkness. The fluorescence at an excitation wavelength of 544 nm and an emission wavelength of 620 nm was read in the SpectraMax microplate reader. The values were transformed to microgram equivalents of dextran based on a calibration curve using 25 μL of serial dilutions of dextran MW 70000 from *Leuconostoc mesenteroides* (Sigma-Aldrich). The quantity of polysaccharides was normalized to the total biomass in the same sample and expressed as the ratio between the sample and the control (no antimicrobial added).

Pharmacodynamic curves and combination analysis. GraphPad Prism 8.0.2 (GraphPad Software, San Diego, CA) was used to draw concentration-response curves, calculate pharmacodynamic parameters, and run statistical analyses of data obtained with single drugs.

Data were used to fit a 4-parameter logistic or Hill curve (equation 1):

$$y = E_{\max} + \frac{E_{\min} - E_{\max}}{1 + 10^{(\log EC_{50} - x) \times h}} \quad (1)$$

where E_{\max} is the maximal effect of the drug and thus the horizontal asymptote at the lowest y value, E_{\min} is the minimal effect of the drug, EC_{50} is the concentration needed to reach an effect halfway between E_{\max} and E_{\min} (inflection point of the curve), and h is the Hill factor. The pharmacodynamic parameters E_{\max} and $C_{-1\log}$ or $C_{-90\%}$ (defined as the concentration required to observe a 90% reduction in total culturable cells [$1 \log_{10}$ reduction] or biomass) were calculated from the equation of the curve.

Synergy (increased effect) or antagonism (decreased effect) for drug combinations was determined using the highest-single-agent model of the BIGL 1.4.3 package for R 3.6.2 (68, 69). Contour graphs were plotted using the plotrix 3.7-7 package (70). Briefly, the highest-single-agent model determines if the effect of a drug combination is greater than the effects produced by its single components (32). A schematic overview of the workflow and the script used in R can be found in Fig. S9 and S10, respectively. An expected additive effect (\hat{E}_{AB}) is calculated as the largest effect, and thus the largest reduction and lower value, of the drugs used alone at a given pair of concentrations (E_A and E_B) as detailed in equation 2. The effects of both drugs alone were extrapolated from the fitted pharmacodynamic curve.

$$\hat{E}_{AB} = \min(E_A, E_B) \quad (2)$$

As detailed by Van der Borghet et al., two statistical tests based on the analysis of variances are run to compare \hat{E}_{AB} with the experimental combinatory effect (E_{AB}) (68). The first test determines if the overall E_{AB} fits the \hat{E}_{AB} additive model. If there is at least a significant difference, the second test identifies which E_{AB} deviates significantly from \hat{E}_{AB} and if it corresponds to synergy (increased effect) or antagonism (decreased effect).

Confocal microscopy (live/dead staining). Biofilms grown on coupons were imaged after incubation with antimicrobials alone or in combination. Two hundred microliters of a mixture of FilmTracer Live/Dead (Syto9 0.01 mM, propidium iodide 0.06 mM; Invitrogen, Carlsbad, CA) and 50 mg/L calcofluor white (Sigma-Aldrich) in water was added very gently on top of the biofilms and incubated 30 min in darkness. Excess dye was rinsed off with water, and excess liquid was removed with absorbent paper. Coupons were mounted with Dako mounting oil (Agilent, Santa Clara, CA) and a glass coverslip. Z-stack pictures of the stained biofilms were taken with an AxioImager.z1-ApoTome microscope (Carl Zeiss, Oberkochen, Germany) through a multiaquisition from the top to the bottom of the biofilm. The means of filter sets (excitation/emission) were as follows: blue, 365/450 nm; green, 460/550 nm; and red, 535/590 nm. Pictures were analyzed and converted to maximal-intensity projections with AxioVision release 4.8.2.0 (Carl Zeiss).

Data availability. All raw data will be made available from the corresponding author upon request.

SUPPLEMENTAL MATERIAL

Supplemental material is available online only.

SUPPLEMENTAL FILE 1, PDF file, 1.5 MB.

ACKNOWLEDGMENTS

We thank Alix Mangin for his dedicated technical assistance, Caroline Bouzin (IREC, UCLouvain, Brussels, Belgium) for advice and support in imaging studies, and Vallo Varik (EMBL, Heidelberg, Germany) for his advice in the analysis of the combinatory therapy.

A.R.-S. was funded by the Orthenzy project, Win²Wal program from Région Wallonne, Belgium. H.P. was funded by Fonds pour la Recherche dans l'Industrie et l'Agriculture (FRIA) from FRS-FNRS. F.V.B. is a research director from the Belgian Fonds de la Recherche Scientifique FRS-FNRS. This work was supported by the Région Wallonne (Win²Wal program) and the Belgian FRS-FNRS (grant J.0162.19).

We declare no conflict of interest.

REFERENCES

- Arciola CR, Campoccia D, Montanaro L. 2018. Implant infections: adhesion, biofilm formation and immune evasion. *Nat Rev Microbiol* 16: 397–409. <https://doi.org/10.1038/s41579-018-0019-y>.
- Hall CW, Mah T-F. 2017. Molecular mechanisms of biofilm-based antibiotic resistance and tolerance in pathogenic bacteria. *FEMS Microbiol Rev* 41:276–301. <https://doi.org/10.1093/femsre/fux010>.
- Crabbé A, Jensen PØ, Bjarnsholt T, Coenye T. 2019. Antimicrobial tolerance and metabolic adaptations in microbial biofilms. *Trends Microbiol* 27:850–863. <https://doi.org/10.1016/j.tim.2019.05.003>.
- Fisher RA, Gollan B, Helaine S. 2017. Persistent bacterial infections and persister cells. *Nat Rev Microbiol* 15:453–464. <https://doi.org/10.1038/nrmicro.2017.42>.
- VanEpps JS, Younger JG. 2016. Implantable device-related infection. *Shock* 46:597–608. <https://doi.org/10.1097/SHK.0000000000000692>.
- Darouiche RO. 2004. Treatment of infections associated with surgical implants. *N Engl J Med* 350:1422–1429. <https://doi.org/10.1056/NEJMra035415>.
- Weiner-Lastinger LM, Abner S, Edwards JR, Kallen AJ, Karlsson M, Magill SS, Pollock D, See I, Soe MM, Walters MS, Dudeck MA. 2020. Antimicrobial-resistant pathogens associated with adult healthcare-associated infections: summary of data reported to the National Healthcare Safety Network, 2015–2017. *Infect Control Hosp Epidemiol* 41:1–18. <https://doi.org/10.1017/ice.2019.296>.
- Percival SL, Suleman L, Vuotto C, Donelli G. 2015. Healthcare-associated infections, medical devices and biofilms: risk, tolerance and control. *J Med Microbiol* 64:323–334. <https://doi.org/10.1099/jmm.0.000032>.
- Jakobsen TH, Eickhardt SR, Gheorghie AG, Stenqvist C, Sønderholm M, Stavnsberg C, Jensen PØ, Odgaard A, Whiteley M, Moser C, Hvolris J, Hougen HP, Bjarnsholt T. 2018. Implants induce a new niche for microbiomes. *APMIS* 126:685–692. <https://doi.org/10.1111/apm.12862>.
- Parikh MS, Antony S. 2016. A comprehensive review of the diagnosis and management of prosthetic joint infections in the absence of positive cultures. *J Infect Public Health* 9:545–556. <https://doi.org/10.1016/j.jiph.2015.12.001>.
- Arvanitis M, Mylonakis E. 2015. Fungal-bacterial interactions and their relevance in health. *Cell Microbiol* 17:1442–1446. <https://doi.org/10.1111/cmi.12493>.
- Kojic EM, Darouiche RO. 2004. Candida infections of medical devices. *Clin Microbiol Rev* 17:255–267. <https://doi.org/10.1128/CMR.17.2.255-267.2004>.
- Nace J, Siddiqi A, Talmo CT, Chen AF. 2019. Diagnosis and management of fungal periprosthetic joint infections. *J Am Acad Orthop Surg* 27:1–15. <https://doi.org/10.5435/JAAOS-D-18-00331>.
- Tan TL, Kheir MM, Tan DD, Parvizi J. 2016. Polymicrobial periprosthetic joint infections: outcome of treatment and identification of risk factors. *J Bone Joint Surg* 98:2082–2088. <https://doi.org/10.2106/JBJS.15.01450>.
- Rodrigues ME, Gomes F, Rodrigues CF. 2020. Candida spp./bacteria mixed biofilms. *J Fungi* 6:5. <https://doi.org/10.3390/jof6010005>.
- Kong EF, Tsui C, Kucharíková S, Andes D, Van Dijck P, Jabra-Rizk MA. 2016. Commensal protection of *Staphylococcus aureus* against antimicrobials by *Candida albicans* biofilm matrix. *mBio* 7:e01365-16. <https://doi.org/10.1128/mBio.01365-16>.
- Vila T, Kong EF, Montelongo-Jauregui D, Van Dijck P, Shetty AC, McCracken C, Bruno VM, Jabra-Rizk MA. 2021. Therapeutic implications of *C. albicans*-*S. aureus* mixed biofilm in a murine subcutaneous catheter model of polymicrobial infection. *Virulence* 12:835–851. <https://doi.org/10.1080/21505594.2021.1894834>.
- Adam B, Baillie GS, Douglas LJ. 2002. Mixed species biofilms of *Candida albicans* and *Staphylococcus epidermidis*. *J Med Microbiol* 51:344–349. <https://doi.org/10.1099/0022-1317-51-4-344>.
- De Brucker K, Tan Y, Vints K, De Cremer K, Braem A, Verstraeten N, Michiels J, Vleugels J, Cammue BPA, Thevissen K. 2015. Fungal β -1,3-glucan increases ofloxacin tolerance of *Escherichia coli* in a polymicrobial *E. coli*/*Candida albicans* biofilm. *Antimicrob Agents Chemother* 59:3052–3058. <https://doi.org/10.1128/AAC.04650-14>.
- Ruiz-Sorribas A, Poilvache H, Kamarudin NHN, Braem A, Van Bambeke F. 2021. In vitro polymicrobial inter-kingdom three-species biofilm model: influence of hyphae on biofilm formation and bacterial physiology. *Biofouling* 37:481–493. <https://doi.org/10.1080/08927014.2021.1919301>.
- Donnenberg MS. 2015. Enterobacteriaceae, p 2503–2517. In Bennett JE, Dolin R, Blaser MJ (ed), Mandell, Douglas, and Bennett's principles and practice of infectious diseases, 8th ed. Elsevier, Philadelphia, PA.
- Edwards JE. 2015. *Candida* species, p 2879–2894. In Bennett JE, Dolin R, Blaser MJ (ed), Mandell, Douglas, and Bennett's principles and practice of infectious diseases, 8th ed. Elsevier, Philadelphia, PA.
- Osmon DR, Berbari EF, Berendt AR, Lew D, Zimmerli W, Steckelberg JM, Rao N, Hanssen A, Wilson WR, Infectious Diseases Society of America. 2013. Diagnosis and management of prosthetic joint infection: clinical practice guidelines by the Infectious Diseases Society of America. *Clin Infect Dis* 56:1–25. <https://doi.org/10.1093/cid/cis966>.
- Moczygomba LR, Frei CR, Burgess DS. 2004. Pharmacodynamic modeling of carbapenems and fluoroquinolones against bacteria that produce extended-spectrum beta-lactamases. *Clin Ther* 26:1800–1807. <https://doi.org/10.1016/j.clinthera.2004.11.009>.
- Sawistowska-Schröder ET, Kerridge D, Perry H. 1984. Echinocandin inhibition of 1,3- β -D-glucan synthase from *Candida albicans*. *FEBS Lett* 173: 134–138. [https://doi.org/10.1016/0014-5793\(84\)81032-7](https://doi.org/10.1016/0014-5793(84)81032-7).
- Douglas CM, D'ippolito JA, Shei GJ, Meinz M, Onishi J, Marrinan JA, Li W, Abruzzo GK, Flatterly A, Bartizal K, Mitchell A, Kurtz MB. 1997. Identification of the FKS1 gene of *Candida albicans* as the essential target of 1,3-beta-D-glucan synthase inhibitors. *Antimicrob Agents Chemother* 41: 2471–2479. <https://doi.org/10.1128/AAC.41.11.2471>.
- Itoh Y, Rice JD, Goller C, Pannuri A, Taylor J, Meisner J, Beveridge TJ, Preston JF, Romeo T. 2008. Roles of pgaABCD genes in synthesis, modification, and export of the *Escherichia coli* biofilm adhesin poly-beta-1,6-N-acetyl-D-glucosamine. *J Bacteriol* 190:3670–3680. <https://doi.org/10.1128/JB.01920-07>.
- Whitfield GB, Marmont LS, Howell PL. 2015. Enzymatic modifications of exopolysaccharides enhance bacterial persistence. *Front Microbiol* 6:471. <https://doi.org/10.3389/fmicb.2015.00471>.
- Siala W, Kucharíková S, Braem A, Vleugels J, Tulkens PM, Mingeot-Leclercq M-P, Van Dijck P, Van Bambeke F. 2016. The antifungal caspofungin increases fluoroquinolone activity against *Staphylococcus aureus* biofilms by inhibiting N-acetylglucosamine transferase. *Nat Commun* 7: 13286. <https://doi.org/10.1038/ncomms13286>.
- Rogiers O, Holtappels M, Siala W, Lamkanfi M, Van Bambeke F, Lagrou K, Van Dijck P, Kucharíková S. 2018. Anidulafungin increases the antibacterial activity of tigecycline in polymicrobial *Candida albicans*/*Staphylococcus aureus* biofilms on intraperitoneally implanted foreign bodies. *J Antimicrob Chemother* 73:2806–2814. <https://doi.org/10.1093/jac/dky246>.
- Kissoyan KAB, Bazzi W, Hadi U, Matar GM. 2016. The inhibition of *Pseudomonas aeruginosa* biofilm formation by micafungin and the enhancement of antimicrobial agent effectiveness in BALB/c mice. *Biofouling* 32: 779–786. <https://doi.org/10.1080/08927014.2016.1199021>.
- Fouquier J, Guedj M. 2015. Analysis of drug combinations: current methodological landscape. *Pharmacol Res Perspect* 3:e00149. <https://doi.org/10.1002/prp2.149>.
- Lubasch A, Keller I, Borner K, Koeppe P, Lode H. 2000. Comparative pharmacokinetics of ciprofloxacin, gatifloxacin, grepafloxacin, levofloxacin, trovafloxacin, and moxifloxacin after single oral administration in healthy volunteers. *Antimicrob Agents Chemother* 44:2600–2603. <https://doi.org/10.1128/AAC.44.10.2600-2603.2000>.
- Würthwein G, Cornely OA, Trame MN, Vehreschild JJ, Vehreschild MJGT, Farowski F, Müller C, Boos J, Hempel G, Hallek M, Groll AH. 2013. Population pharmacokinetics of escalating doses of caspofungin in a phase II

- study of patients with invasive aspergillosis. *Antimicrob Agents Chemother* 57:1664–1671. <https://doi.org/10.1128/AAC.01912-12>.
35. Dandekar PK, Maglio D, Sutherland CA, Nightingale CH, Nicolau DP. 2003. Pharmacokinetics of meropenem 0.5 and 2 g every 8 hours as a 3-hour infusion. *Pharmacotherapy* 23:988–991. <https://doi.org/10.1592/phco.23.8.988.32878>.
 36. Vandecandelaere I, Van Nieuwerburgh F, Deforce D, Coenye T. 2017. Metabolic activity, urease production, antibiotic resistance and virulence in dual species biofilms of *Staphylococcus epidermidis* and *Staphylococcus aureus*. *PLoS One* 12:e0172700. <https://doi.org/10.1371/journal.pone.0172700>.
 37. Delattin N, De Brucker K, Vandamme K, Meert E, Marchand A, Chaltin P, Cammue BPA, Thevissen K. 2014. Repurposing as a means to increase the activity of amphotericin B and caspofungin against *Candida albicans* biofilms. *J Antimicrob Chemother* 69:1035–1044. <https://doi.org/10.1093/jac/dkt449>.
 38. Tavernier S, Crabbé A, Hacıoglu M, Stuer L, Henry S, Rigole P, Dhondt I, Coenye T. 2017. Community composition determines activity of antibiotics against multispecies biofilms. *Antimicrob Agents Chemother* 61:1–12. <https://doi.org/10.1128/AAC.00302-17>.
 39. Qu Y, Locock K, Verma-Gaur J, Hay ID, Meagher L, Traven A. 2016. Searching for new strategies against polymicrobial biofilm infections: guanidylated polymethacrylates kill mixed fungal/bacterial biofilms. *J Antimicrob Chemother* 71:413–421. <https://doi.org/10.1093/jac/dkv334>.
 40. Salem AH, Elkhatib WF, Ahmed GF, Noreddin AM. 2010. Pharmacodynamics of moxifloxacin versus vancomycin against biofilms of methicillin-resistant *Staphylococcus aureus* and *epidermidis* in an in vitro model. *J Chemother* 22:238–242. <https://doi.org/10.1179/joc.2010.22.4.238>.
 41. Diaz Iglesias Y, Wilms T, Vanbever R, Van Bambeke F. 2019. Activity of antibiotics against *Staphylococcus aureus* in an in vitro model of biofilms in the context of cystic fibrosis: influence of the culture medium. *Antimicrob Agents Chemother* 63:1–14. <https://doi.org/10.1128/AAC.00602-19>.
 42. Grossman TH, O'Brien W, Kerstein KO, Sutcliffe JA. 2015. Eravacycline (TP-434) is active in vitro against biofilms formed by uropathogenic *Escherichia coli*. *Antimicrob Agents Chemother* 59:2446–2449. <https://doi.org/10.1128/AAC.04967-14>.
 43. Malchikova A, Klyasova G. 2021. In vitro activity of anidulafungin, caspofungin, fluconazole and amphotericin B against biofilms and planktonic forms of *Candida* species isolated from blood culture in patients with hematological malignancies. *J Med Mycol* 31:1–6. <https://doi.org/10.1016/j.mycmed.2021.101162>.
 44. Sumiyoshi M, Miyazaki T, Makau JN, Mizuta S, Tanaka Y, Ishikawa T, Makimura K, Hirayama T, Takazono T, Saijo T, Yamaguchi H, Shimamura S, Yamamoto K, Imamura Y, Sakamoto N, Obase Y, Izumikawa K, Yanagihara K, Kohno S, Mukae H. 2020. Novel and potent antimicrobial effects of caspofungin on drug-resistant *Candida* and bacteria. *Sci Rep* 10:17745. <https://doi.org/10.1038/s41598-020-74749-8>.
 45. Ozcan Keceli S, Budak F, Willke A, Filiz S, Costur P, Dalcik H. 2006. Efficacies of caspofungin and a combination of caspofungin and meropenem in the treatment of murine disseminated candidiasis. *APMIS* 114:829–836. https://doi.org/10.1111/j.1600-0463.2006.apm_450.x.
 46. Aşkın Keçeli S, Willke A, Tamer GS, Boral OB, Sonmez N, Çağatay P. 2014. Interaction between caspofungin or voriconazole and cefoperazone-sulbactam or piperacillin-tazobactam by in vitro and in vivo methods. *APMIS* 122:412–417. <https://doi.org/10.1111/apm.12159>.
 47. Isnard C, Hernandez SB, Guérin F, Joalland F, Goux D, Gravey F, Auzou M, Enot D, Meignen P, Giard J-C, Cava F, Cattoir V. 2020. Unexpected cell wall alteration-mediated bactericidal activity of the antifungal caspofungin against vancomycin-resistant *Enterococcus faecium*. *Antimicrob Agents Chemother* 64:e01261-20. <https://doi.org/10.1128/AAC.01261-20>.
 48. Konopka JB. 2012. N-acetylglucosamine functions in cell signaling. *Scientifica (Cairo)* 2012:1–15. <https://doi.org/10.6064/2012/489208>.
 49. Wang X, Preston JF, Romeo T. 2004. The pgaABCD locus of *Escherichia coli* promotes the synthesis of a polysaccharide adhesin required for biofilm formation. *J Bacteriol* 186:2724–2734. <https://doi.org/10.1128/JB.186.9.2724-2734.2004>.
 50. Hoble L, Harkins C, MacPhee CE, Stanley-Wall NR. 2015. Giving structure to the biofilm matrix: an overview of individual strategies and emerging common themes. *FEMS Microbiol Rev* 39:649–669. <https://doi.org/10.1093/femsre/fuv015>.
 51. Karygianni L, Ren Z, Koo H, Thurnheer T. 2020. Biofilm matrixome: extracellular components in structured microbial communities. *Trends Microbiol* 28:668–681. <https://doi.org/10.1016/j.tim.2020.03.016>.
 52. Tasse J, Trouillet-Assant S, Josse J, Martins-Simões P, Valour F, Langlois-Jacques C, Badel-Berchoux S, Provot C, Bernardi T, Ferry T, Laurent F. 2018. Association between biofilm formation phenotype and clonal lineage in *Staphylococcus aureus* strains from bone and joint infections. *PLoS One* 13:e0200064. <https://doi.org/10.1371/journal.pone.0200064>.
 53. Schiebel J, Böhm A, Nitschke J, Burdukiewicz M, Weinreich J, Ali A, Roggenbuck D, Rödiger S, Schierack P. 2017. Genotypic and phenotypic characteristics associated with biofilm formation by human clinical *Escherichia coli* isolates of different pathotypes. *Appl Environ Microbiol* 83:e01660-17. <https://doi.org/10.1128/AEM.01660-17>.
 54. Dunn MJ, Fillinger RJ, Anderson LM, Anderson MZ. 2020. Automated quantification of *Candida albicans* biofilm-related phenotypes reveals additive contributions to biofilm production. *NPJ Biofilms Microbiomes* 6:36. <https://doi.org/10.1038/s41522-020-00149-5>.
 55. Poilvache H, Ruiz-Sorribas A, Cornu O, Van Bambeke F. 2021. In vitro study of the synergistic effect of an enzyme cocktail and antibiotics against biofilms in a prosthetic joint infection model. *Antimicrob Agents Chemother* 65:e01699-20. <https://doi.org/10.1128/AAC.01699-20>.
 56. Carbone A, Cascioferro S, Parrino B, Carbone D, Pecoraro C, Schillaci D, Cusimano MG, Cirrincione G, Diana P. 2020. Thiazole analogues of the marine alkaloid nortopsentin as inhibitors of bacterial biofilm formation. *Molecules* 26:81. <https://doi.org/10.3390/molecules26010081>.
 57. Gilbert-Girard S, Savijoki K, Yli-Kauhalauma J, Fallarero A. 2020. Optimization of a high-throughput 384-well plate-based screening platform with *Staphylococcus aureus* ATCC 25923 and *Pseudomonas aeruginosa* ATCC 15442 biofilms. *Int J Mol Sci* 21:3034. <https://doi.org/10.3390/ijms21093034>.
 58. Song H, Lou N, Liu J, Xiang H, Shang D. 2021. Label-free quantitative proteomic analysis of the inhibition effect of *Lactobacillus rhamnosus* GG on *Escherichia coli* biofilm formation in co-culture. *Proteome Sci* 19:4. <https://doi.org/10.1186/s12953-021-00172-0>.
 59. Khan SN, Khan S, Iqbal J, Khan R, Khan AU. 2017. Enhanced killing and anti-biofilm activity of encapsulated cinnamaldehyde against *Candida albicans*. *Front Microbiol* 8:1641. <https://doi.org/10.3389/fmicb.2017.01641>.
 60. Pangprasit N, Sriphanasuvan A, Suriyathaporn W, Pikuksaew S, Bernard JK, Chairai W. 2020. Antibacterial activities of acetic acid against major and minor pathogens isolated from mastitis in dairy cows. *Pathogens* 9:961–966. <https://doi.org/10.3390/pathogens9110961>.
 61. Hernández SB, Cota I, Ducret A, Aussel L, Casadesús J. 2012. Adaptation and preadaptation of *Salmonella enterica* to bile. *PLoS Genet* 8:e1002459. <https://doi.org/10.1371/journal.pgen.1002459>.
 62. Clinical and Laboratory Standards Institute. 2018. Methods for dilution antimicrobial susceptibility tests for bacteria that grow aerobically, 11th ed. CLSI, Wayne, PA.
 63. Arendrup MC, Meletiadi J, Mouton JW, Lagrou K, Hamal P, Guinea J, Eucast AFST. 2020. Method for the determination of broth dilution minimum inhibitory concentrations of antifungal agents for yeasts. EUCAST E.DEF 7.3.2. https://www.eucast.org/astoffungi/methodsinantifungalsusceptibilitytesting/susceptibility_testing_of_yeasts/.
 64. BioSurface Technologies Co. 2021. CDC Biofilm Reactor® (CBR) operator's manual.
 65. Pembrey RS, Marshall KC, Schneider RP. 1999. Cell surface analysis techniques: what do cell preparation protocols do to cell surface properties? *Appl Environ Microbiol* 65:2877–2894. <https://doi.org/10.1128/AEM.65.7.2877-2894.1999>.
 66. Randrianjatovo-Gbalou I, Girbal-Neuhauser E, Marcato-Romain C-E. 2016. Quantification of biofilm exopolysaccharides using an in situ assay with periodic acid-Schiff reagent. *Anal Biochem* 500:12–14. <https://doi.org/10.1016/j.ab.2016.01.008>.
 67. Kilcoyne M, Gerlach JQ, Farrell MP, Bhavanandan VP, Joshi L. 2011. Periodic acid-Schiff's reagent assay for carbohydrates in a microtiter plate format. *Anal Biochem* 416:18–26. <https://doi.org/10.1016/j.ab.2011.05.006>.
 68. Van der Borgh K, Tourny A, Bagdziunas R, Thas O, Nazarov M, Turner H, Verbist B, Ceulemans H. 2017. BIGL: Biochemically Intuitive Generalized Loewe null model for prediction of the expected combined effect compatible with partial agonism and antagonism. *Sci Rep* 7:17935. <https://doi.org/10.1038/s41598-017-18068-5>.
 69. R Core Team. 2019. R: a language and environment for statistical computing. R Foundation for Statistical Computing, Vienna, Austria.
 70. Lemon J. 2006. Plotrix: a package in the red light district of R. *R-News* 6:8–12.

1 **Pharmacodynamics of Moxifloxacin, Meropenem, Caspofungin and Combinations**
2 **Against In Vitro Polymicrobial Inter-kingdom Biofilms**

3 Albert Ruiz-Sorribas ^a, Hervé Poilvache ^{bc}, Françoise Van Bambeke ^a

4 ^a Pharmacologie cellulaire et moléculaire, Louvain Drug Research Institute, Université
5 catholique de Louvain, Brussels, Belgium.

6 ^b Laboratoire de neuro musculo squelettique, Institut de Recherche Expérimentale et
7 Clinique, Université catholique de Louvain, Brussels, Belgium.

8 ^c Orthopaedic surgery department, Cliniques Universitaires Saint-Luc, Brussels, Belgium.

9 Corresponding author: Françoise Van Bambeke (francoise.vanbambeke@uclouvain.be)

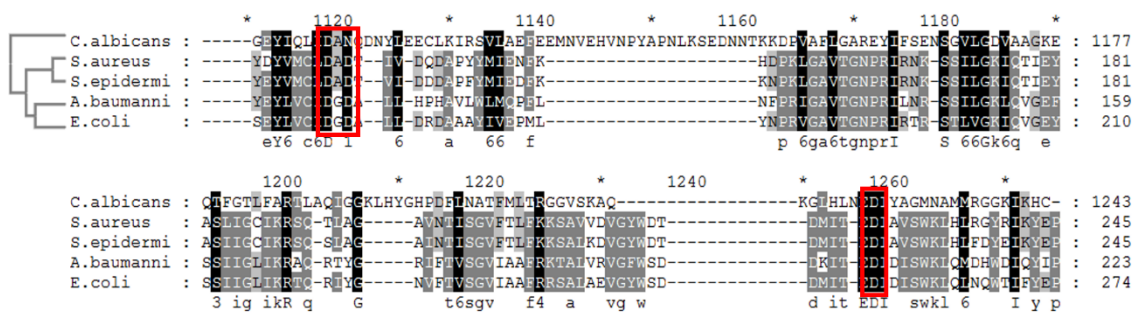
10

11

12 **Supplementary material**

13 **Figure S1. A:** Multiple protein sequence alignment and dendrogram of *C. albicans* Gsc1,
 14 *S. aureus* IcaA, *S. epidermidis* IcaA, *Acinetobacter baumannii* PgaC and *E. coli* PgaC.
 15 The highly conserved Asp132-x-Asp134 and Asp227 (in *S. aureus*) are part of the
 16 predicted catalytic site. The sequence alignment highlights (red boxes) the fact that
 17 residues making part of the predicted catalytic site Asp132-x-Asp134 and Asp227 (in
 18 *S. aureus*) are highly conserved. B: Percentage identity matrix.

19 **A.**

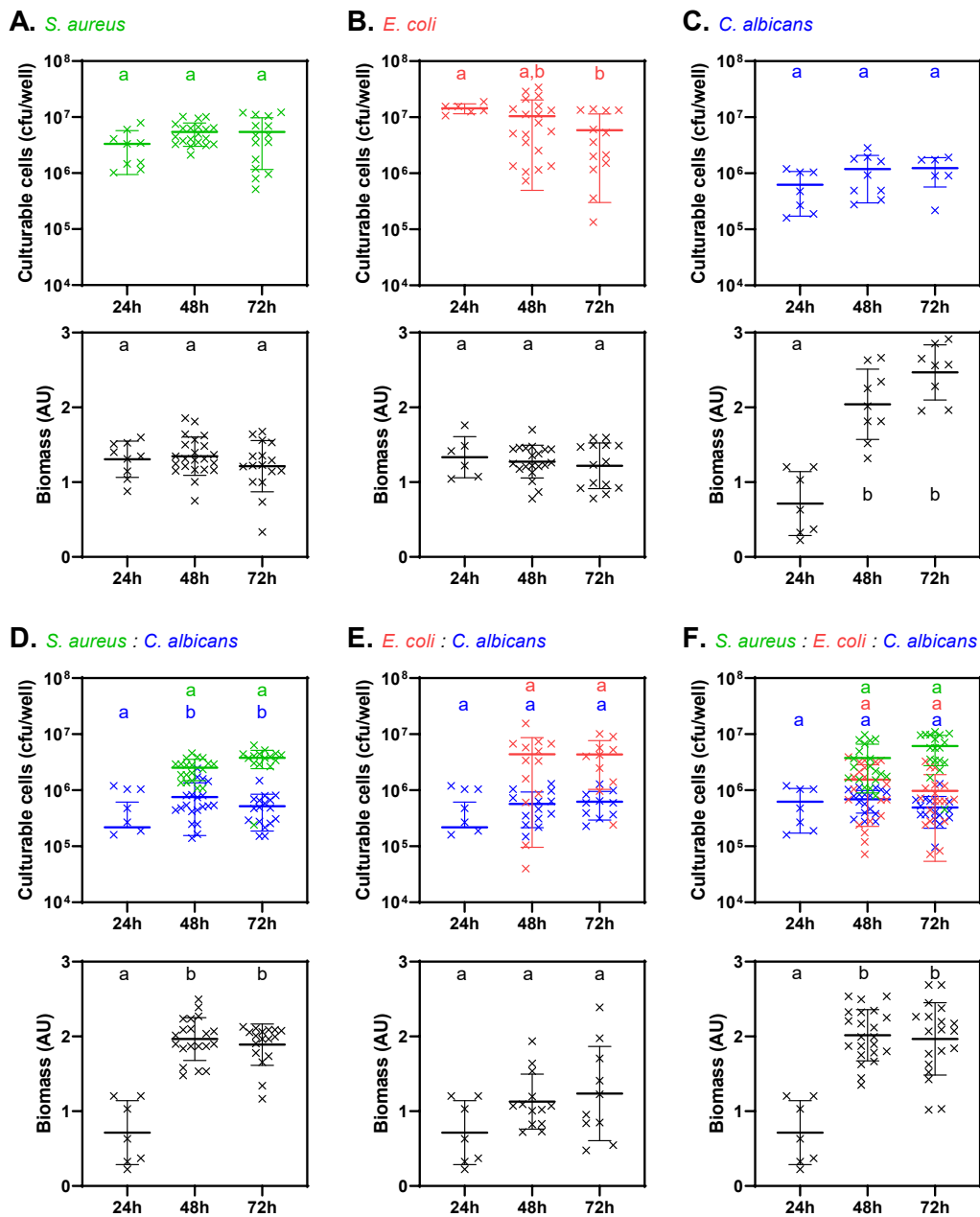


21 **B.**

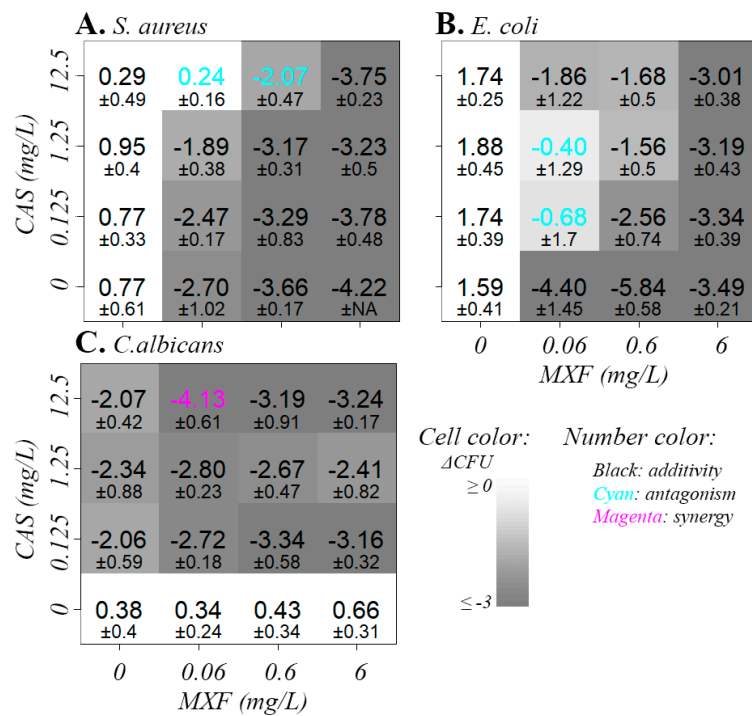
	Gsc1 (<i>C. albicans</i>)	IcaA (<i>S. aureus</i>)	IcaA (<i>S. epidermidis</i>)	PgaC (<i>E. coli</i>)
IcaA (<i>S. aureus</i>)	16.71			
IcaA (<i>S. epidermidis</i>)	18.33	79.13		
PgaC (<i>E. coli</i>)	15.5	38.69	37.96	
PgaC (<i>A. baumannii</i>)	16.39	39.28	39.79	54.64

22

23 **Figure S2.** Evolution over time of cultivable cells and biomass in control biofilms (run
 24 in parallel with biofilms were exposed to single or combined drugs). A-C: single-species
 25 biofilms of *S. aureus*, *E. coli*, and *C. albicans*, respectively; D-E: dual-species biofilms
 26 of *S.aureus*:*C.albicans* and *E.coli*:*C.albicans*; F: three-species biofilm. Each point
 27 corresponds to an independent biological replicate. N=7-22. Statistical analysis: different
 28 letters: significant difference (p -value<0.05; one-way ANOVA, post-Tukey test).



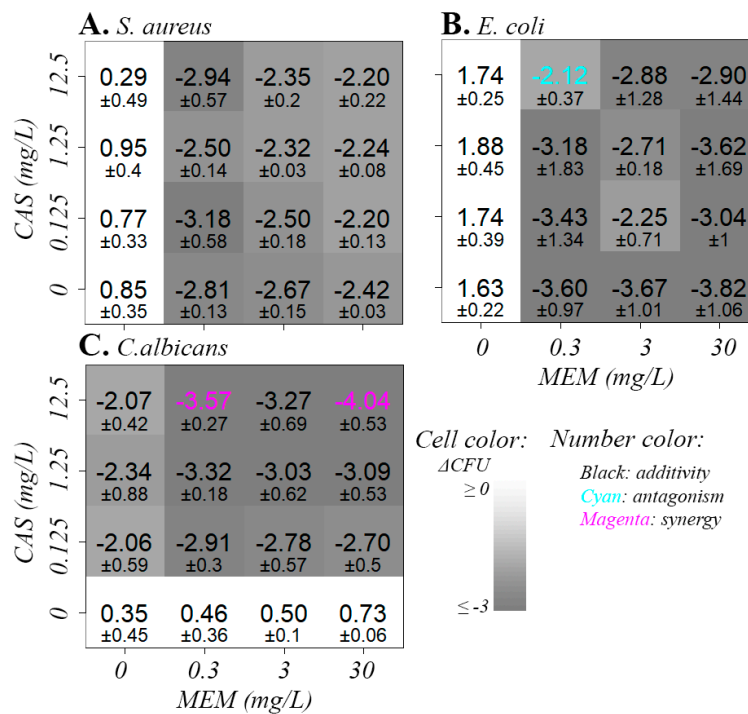
30 **Figure S3.** Effect (average and SD) of the combination moxifloxacin / caspofungin after
 31 24 h incubation with planktonic cultures and its synergy/antagonism (increased/decreased
 32 effect). Data are expressed as $\Delta\log_{10}$ cfu/well. Each drug is used at three selected
 33 concentrations; data for single drugs at the concentrations used in combination are
 34 repeated for clarity. Cells: effect in grey scale (darker means more effect). Black numbers:
 35 additivity (no interaction); magenta numbers: increased effect (synergy; p-value<0.05);
 36 cyan numbers: decreased effect (antagonism; p-value<0.05). X-axis: [moxifloxacin] = 0,
 37 0.06, 0.6, 6 mg/L. Y-axis: [caspofungin] = 0, 0.125, 1.25, 12.5 mg/L.



38

39

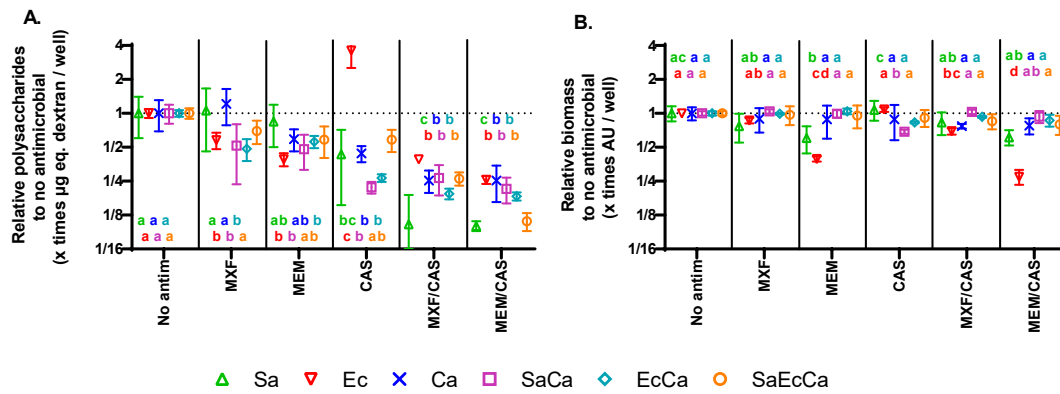
40 **Figure S4.** Effect (average and SD) of the combination meropenem / caspofungin after
 41 24 h incubation with planktonic cultures and its synergy/antagonism (increased/decreased
 42 effect). Data are expressed as $\Delta\log_{10}$ cfu/well. Each drug is used at three selected
 43 concentrations; data for single drugs at the concentrations used in combination are
 44 repeated for clarity. Cells: effect in grey scale (darker means more effect). Black numbers:
 45 additivity (no interaction); magenta numbers: increased effect (synergy; p-value<0.05);
 46 cyan numbers: decreased effect (antagonism; p-value<0.05). X-axis: [meropenem] = 0,
 47 0.3, 3, 30 mg/L. Y-axis: [caspofungin] = 0, 0.125, 1.25, 12.5 mg/L.



48

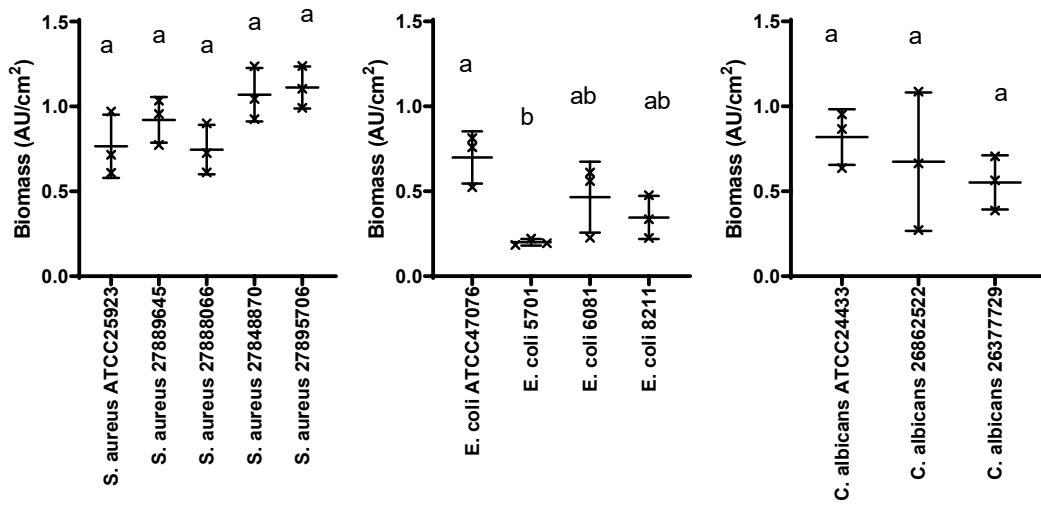
49

50 **Figure S5.** Relative quantification of polysaccharides (A) and biomass (B) after
 51 incubation with antimicrobials, expressed as the ratio with the value measured in the
 52 corresponding control (no antimicrobial added). The data is complementary to Figure 8.
 53 N = 3-6. Statistical analysis: different letters of same colour denote significant difference
 54 ($p < 0.05$; one-way non-parametric ANOVA, Tukey post-test). Sa: *S. aureus*. Ec: *E. coli*.
 55 Ca: *C. albicans*. Ec:Ca, Sa:Ca, Sa:Ec:Ca biofilm: dual- or three-species biofilms. MXF:
 56 moxifloxacin 6 mg/L; MEM: meropenem 30 mg/L; CAS: caspofungin 12.5 mg/L.

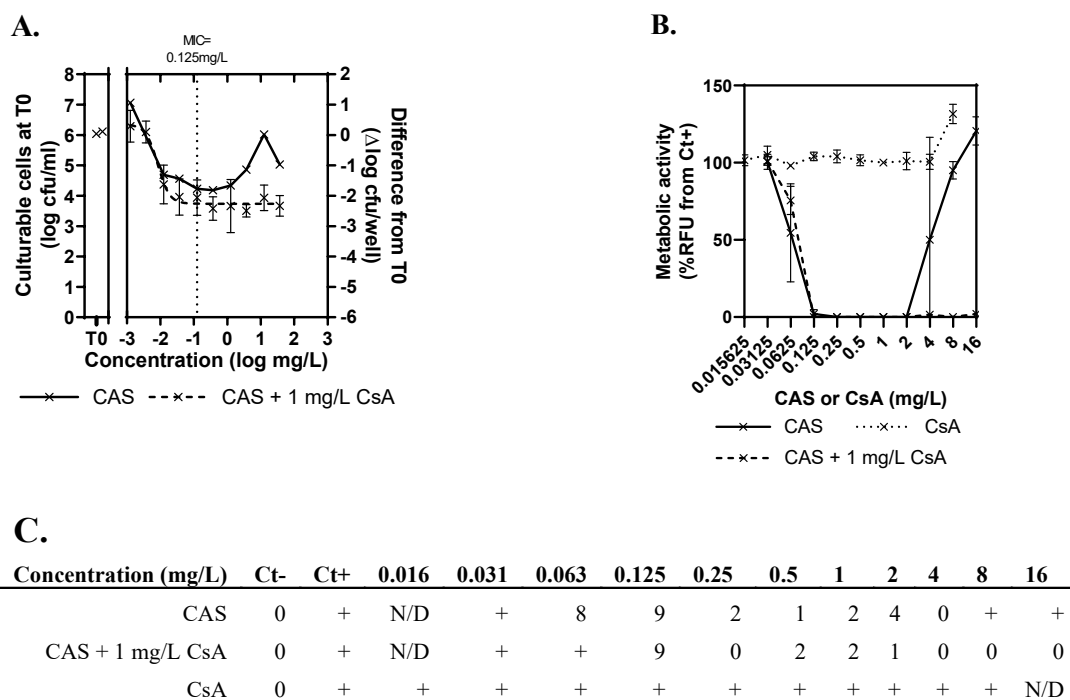


57

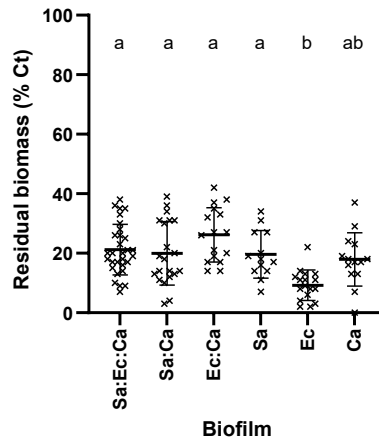
58 **Figure S6.** Comparison of biofilm formation on Ti coupons by reference and clinical
 59 strains, as evaluated by quantification of the biomass using crystal violet staining. The
 60 clinical isolates were kindly provided by Prof Hector Rodriguez-Villalobos (Clinical
 61 Microbiology Department, *cliniques universitaires Saint Luc*, Brussels, Belgium). Each
 62 point represents a coupon. Different letters represent a significant difference (p-value <
 63 0.05; non-parametric One-way ANOVA, post-Tukey test).



65 **Figure S7.** Paradoxical growth of *C. albicans* exposed to caspofungin in RPMI + 20mM
66 Hepes. A: planktonic growth in tubes. B: metabolic activity in 96w microplates, assessed
67 by the fluorescence of resorufin (Ex560 nm/Em590nm) after 30 min incubation with
68 0.01g/L resazurin. C: cultivability in 96w microplates, assessed by the number of colonies
69 on a dot spot with 10 μ L from each well on SGA. +: more colonies than able to distinguish.
70 Cyclosporin A was used to avoid the paradoxical growth at intermediate concentrations
71 of caspofungin. Some authors have reported that intermediate concentrations of
72 echinocandins, roughly between 4 to 32-64 mg/L, induce a change in the cell wall
73 polysaccharides from β -glucan to chitin, which allows the fungus to persist the
74 echinocandins. This is known as the paradoxical effect or growth and, to the best of our
75 knowledge, it has only been observed in vitro and it is limited to some strains (1).
76 Although it is not fully understood, calcineurin-pathway inhibitor molecules, like
77 cyclosporin A, avoid this transition (2, 3). Cyclosporin A has no inhibitory effect on its
78 own against *C. albicans*, *S. aureus* or *E. coli* (MIC >32 mg/L).



80 **Figure S8.** Quality controls of residual biomass after detaching the biofilm from the
81 microtiter plates. Each point represents the average of one experiment. Different letters
82 represent a significant difference (p-value < 0.05; One-way ANOVA, post-Tukey test).

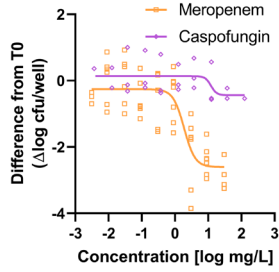


83

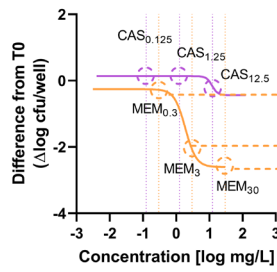
84

85 **Figure S9.** Schematic overview of the Highest Single-Agent model workflow.

1) Fitting concentration-response curves to single drug experiments.



2) Estimating the effect of single drug E_{MEM} and E_{CAS} at given concentrations.



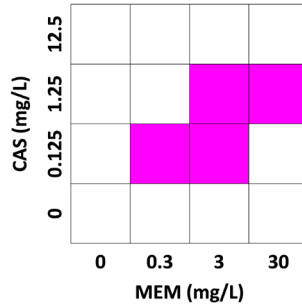
3) Estimating the expected additive effect for the combination at each pair of concentrations according to the highest single agent model $\hat{E}_{MEM/CAS} = \min(E_{MEM}, E_{CAS})$.

		0.3	3	30
12.5	-0.28 ±0.63	-2.07 ±1.32	-2.6 ±1.17	
1.25	-0.28 ±0.63	-2.07 ±1.32	-2.6 ±1.17	
0.125	-0.28 ±0.63	-2.07 ±1.32	-2.6 ±1.17	

4) Obtaining the experimental effect ($E_{MEM/CAS}$) of the combination at each pair of concentrations and of each single agent at the same concentrations in the same experiment.

		0	0.3	3	30
12.5	-0.18 ±0.64	-0.84 ±0.44	-2.82 ±0.48	-3.43 ±0.61	
1.25	0.03 ±0.41	-1.10 ±0.29	-3.53 ±0.21	-4.25 ±0.39	
0.125	0.21 ±0.61	-1.18 ±0.61	-3.23 ±0.55	-3.88 ±0.43	
0	-0.05 ±0.56	-0.45 ±0.83	-2.11 ±1.04	-2.86 ±0.46	

5) Comparing $E_{MEM/CAS}$ (4) vs $\hat{E}_{MEM/CAS}$ (3) to determine if there is a synergy ($E_{MEM/CAS} < \hat{E}_{MEM/CAS}$), antagonism ($E_{MEM/CAS} > \hat{E}_{MEM/CAS}$) or no-interaction ($E_{MEM/CAS} \sim \hat{E}_{MEM/CAS}$).



6) Plotting graphically the effects of each combination of concentrations together with that of each single drug at the same concentration, and report the significant synergy/antagonism by a color code.

		0	0.3	3	30
12.5	-0.18 ±0.64	-0.84 ±0.44	-2.82 ±0.48	-3.43 ±0.61	
1.25	0.03 ±0.41	-1.10 ±0.29	-3.53 ±0.21	-4.25 ±0.39	
0.125	0.21 ±0.61	-1.18 ±0.61	-3.23 ±0.55	-3.88 ±0.43	
0	-0.05 ±0.56	-0.45 ±0.83	-2.11 ±1.04	-2.86 ±0.46	

86

87

88 **Figure S10.** Script used for the highest single-agent analysis for R.

```
89 ##### Synergy analysis #####
90
91 ## Based on:
92 ## https://cran.r-project.org/web/packages/BIGL/vignettes/analysis.html
93
94 ## Packages and setting working directory #####
95
96 install.packages("BIGL", lib = "E:/Packages directory")
97 install.packages("ggplot2", lib = "E:/Packages directory")
98 install.packages("openxlsx", lib = "E:/Packages directory")
99 install.packages("dplyr", lib = "E:/Packages directory")
100 install.packages("plotrix", lib = "E:/Packages directory")
101
102 library(BIGL, lib.loc = "E:/Packages directory")
103 library(ggplot2, lib.loc = "E:/Packages directory")
104 library(openxlsx, lib.loc = "E:/Packages directory")
105 library(dplyr, lib.loc = "E:/Packages directory")
106 library(plotrix, lib.loc = "E:/Packages directory")
107
108 setwd("E:/Working directory")
109
110 ##### Data input #####
111
112 ## The data for the analysis must come in a table with required
113 ## columns "d1", "d2" and "effect" for doses of two compounds and
114 ## observed cell counts respectively. Those titles cannot be changed.
115 ## It is also required a numerical value to identify each
116 ## subexperiment to analyze independently. In this script is called
117 ## "experiment". Other information used in this script is a label
118 ## for the experiment type and for the object of study: "Test",
119 ## "Microorganism" and "Biofilm".
120
121 a1 <- "MXF"
122 a2 <- "CAS"
123 am <- c(a1,a2)
124
125 results.comb <- read.xlsx("R_data.xlsx")
126
127 subset.data <- function(data, i) {
128   subset(data, experiment == i)[c("effect", "d1", "d2")]
129 }
130
131 nExp <- max(results.comb$experiment)
132
133 id.results <- subset(results.comb)[c("Test","Microorganism",
134                                     "Biofilm","experiment")]
135
136 id.results <- unique(id.results)
137 paste.noNA <- function(id, sep=", ") {
138   gsub(", ", sep, toString(id[!is.na(id) & id!=" & id!="NA"]))
139 }
140 sep <- ", "
141 id.results$id <- apply(id.results[, c(1:3)], 1,
142                       paste.noNA, sep=", ")
143
144 sCFU <- seq_len(length(which(id.results$Test == "CFU")))
145 sBiomass <- id.results$experiment[-sCFU]
146
147 ##### Highest Single Agent #####
148
149 data.list <- list()
150 fit.data.list <- list()
151 title.list <- list()
152 HSA.list <- list()
153
154 for (i in seq_len(nExp)) {
155   data <- subset.data(data = results.comb, i)
156   fit.data <- tryCatch({
157     fitMarginals(data, transforms = NULL,
158                 method = "nlsml", names = am)
159   }, warning = function(w) w, error = function(e) e)
160
161   if (inherits(fit.data, c("warning", "error")))
162     fit.data <- tryCatch({
```

```

162     fitMarginals(data, transforms = NULL,
163                 method = "optim", names = am)
164   })
165
166   title <- paste(id.results[i,5])
167
168   HSA <- fitSurface(data, fit.data, method = "model",
169                   null_model = "hsa",
170                   statistic = "both", B.CP = 20,
171                   parallel = FALSE)
172
173   data.list[[i]] <- data
174   fit.data.list[[i]] <- fit.data
175   title.list[[i]] <- title
176   HSA.list[[i]] <- HSA
177 }
178
179 ### Marginal fits graphs #####
180
181 dir.create("Marginal_fits")
182
183 plot.fit.data.list <- list()
184
185 for (i in seq_len(nExp)){
186   plot.fit.data <- plot(fit.data.list[[i]]
187                       )+ ggtitle(title.list[[i]])
188
189   plot.fit.data.list[[i]] <- plot.fit.data
190
191   tiff (filename=paste0("Marginal_fits/Marg_fit_",
192                       a1,a2,"_",i,".tiff"))
193   print(plot.fit.data.list[[i]])
194   dev.off()
195 }
196
197 ### Contour graphs #####
198
199 dir.create("Contour_graphs_HSA")
200
201 tiff(filename = paste0("Contour_graphs_HSA/Contour_",
202                       a1,a2,"_HSA_%.02d.tiff"))
203 for (i in seq_len(nExp)) {
204   contour(HSA.list[[i]],
205          colorPalette = c("blue", "white", "red"),
206          main = title.list[[i]],
207          digits = 3, cutoff = 1,
208          xlab = paste(a1,"(mg/L)"), ylab = paste(a2,"(mg/L)"),
209          plevels = c(0.95,0.99,0.999))
210 }
211 dev.off()
212
213 pdf(paste0("Contour_",a1,a2,"_HSA.pdf"))
214 for (i in seq_len(nExp)) {
215   contour(HSA.list[[i]],
216          colorPalette = c("blue", "white", "red"),
217          main = title.list[[i]],
218          digits = 3, cutoff = 1,
219          xlab = paste(a1,"(mg/L)"), ylab = paste(a2,"(mg/L)"),
220          plevels = c(0.95,0.99,0.999))
221 }
222 dev.off()
223
224 ### Output table with results #####
225
226 desc.eff.list <- list()
227 desc.sd.list <- list()
228 mHSA.eff.sd.syn.list <- list()
229
230 subset.name <- function(data) {
231   subset(data, d1 != 0 & d2 != 0)[c("d1", "d2")]
232 }
233 subset.m <- function(data) {
234   subset(data, data[2] != "NA")[col.name]
235 }
236 check.syn <- function (data, j) {
237   if(data$R[j] < 0) return ("*") else("a")
238 }

```

```

239 define.add <- function(data, j) {
240   if(data$call[j] == "None") return(NA) else(data$check[j])
241 }
242
243 HSA.syn.list <- list()
244
245 for (i in seq_len(nExp)) {
246   desc.eff <- aggregate(effect ~ d1 + d2,
247     data = data.list[[i]], mean)
248   desc.sd <- aggregate(effect ~ d1 + d2, data = data.list[[i]], sd)
249   desc.eff$effect <- round(desc.eff$effect, digits = 2)
250   desc.sd$effect <- round(desc.sd$effect, digits = 2)
251   desc.eff.sd <- cbind.data.frame(desc.eff$d1, desc.eff$d2,
252     paste(desc.eff$effect,
253       desc.sd$effect, sep= " ±"))
254   colnames(desc.eff.sd) <- c("d1", "d2", "effect.sd")
255
256   name <- subset.name(data = desc.eff)
257   col.name <- unique(name$d1)
258   col.name <- c("0", unique(name$d1))
259
260   HSA.syn <- subset(HSA.list[[i]][["maxR"]][["Ymean"]]) [
261     c("d1", "d2", "call", "R")]
262   for(j in seq_len(nrow(HSA.syn))) {
263     HSA.syn$check[j] <- check.syn (data = HSA.syn, j)
264     HSA.syn$check[j] <- define.add (data = HSA.syn, j)
265   }
266   HSA.syn$R <- NULL
267   HSA.syn$call <- NULL
268   HSA.syn$call <- HSA.syn$check
269   HSA.syn$check <- NULL
270   HSA.syn$call <- as.factor(HSA.syn$call)
271
272   HSA.eff.sd.syn <- full_join (desc.eff.sd, HSA.syn,
273     by = c("d1", "d2"))
274   HSA.eff.sd.syn$eff.sd.syn <- apply(HSA.eff.sd.syn[,c(3:4)], 1,
275     paste.noNA, sep=" ")
276   HSA.eff.sd.syn$effect.sd <- NULL
277   HSA.eff.sd.syn$call <- NULL
278
279   mHSA.eff.sd.syn <- reshape(HSA.eff.sd.syn, direction = "wide",
280     idvar = "d2", timevar = "d1")
281   rownames(mHSA.eff.sd.syn) <- mHSA.eff.sd.syn$d2
282   mHSA.eff.sd.syn$d2 <- NULL
283   colnames(mHSA.eff.sd.syn) <- unique(desc.eff.sd$d1)
284
285   mHSA.eff.sd.syn <- as.data.frame(mHSA.eff.sd.syn)
286   mHSA.eff.sd.syn <- subset(mHSA.eff.sd.syn)[col.name]
287   mHSA.eff.sd.syn <- subset.m (data = mHSA.eff.sd.syn)
288
289   desc.eff.list[[i]] <- desc.eff
290   desc.sd.list[[i]] <- desc.sd
291   HSA.syn.list[[i]] <- HSA.syn
292   mHSA.eff.sd.syn.list[[i]] <- mHSA.eff.sd.syn
293 }
294
295 wb <- createWorkbook()
296 addWorksheet(wb, sheetName = paste0(a1, a2, "_HSA"))
297
298 for (i in seq_len(nExp)) {
299   writeData(wb, sheet = paste0(a1, a2, "_HSA"), x = title.list[[i]],
300     xy = c(1, paste(2+7*(i-1)))
301   writeData(wb, sheet = paste0(a1, a2, "_HSA"),
302     x = mHSA.eff.sd.syn.list[[i]],
303     xy = c(2, paste(3+7*(i-1))), rowNames = TRUE,
304     keepNA = TRUE, na.string = "ND")
305 }
306
307 saveWorkbook(wb, file = paste0(a1, "_", a2, ".xlsx"),
308   overwrite = FALSE)
309
310 ### Published graphs #####
311
312 # Need to run previous section before.
313
314 subset.mono <- function(data) {
315   subset(data, d1 == 0 | d2 == 0)[c("d1", "d2")]

```

```

316 }
317
318 mdesc.eff.list <- list()
319 mdesc.sd.list <- list()
320
321 cor.syn <- "magenta"
322 cor.ant <- "cyan"
323 cor.add <- "black"
324 cor.mono <- "black"
325
326 for (i in sCFU){
327   desc.sd.list[[i]]$sd <- paste0("±",desc.sd.list[[i]]$effect)
328   desc.sd.list[[i]]$effect <- NULL
329 }
330
331 for (i in sBiomass){
332   desc.sd.list[[i]]$sd <- paste0("±",round(desc.sd.list[[i]]$effect,
333                                           digits = 1))
334   desc.sd.list[[i]]$effect <- NULL
335 }
336
337 for (i in seq_len(nExp)){
338   mdesc.eff <- reshape(desc.eff.list[[i]], direction = "wide",
339                       idvar = "d2", timevar = "d1")
340   rownames(mdesc.eff) <- mdesc.eff$d2
341   mdesc.eff$d2 <- NULL
342   colnames(mdesc.eff) <- unique(desc.eff.list[[i]]$d1)
343   mdesc.eff <- as.data.frame(mdesc.eff)
344   mdesc.eff <- subset(mdesc.eff)[col.name]
345   mdesc.eff <- subset.m (data = mdesc.eff)
346   mdesc.eff <- as.matrix (mdesc.eff)
347
348   mdesc.sd <- reshape(desc.sd.list[[i]], direction = "wide",
349                      idvar = "d2", timevar = "d1")
350   rownames(mdesc.sd) <- mdesc.sd$d2
351   mdesc.sd$d2 <- NULL
352   colnames(mdesc.sd) <- unique(desc.sd.list[[i]]$d1)
353   mdesc.sd <- as.data.frame(mdesc.sd)
354   mdesc.sd <- subset(mdesc.sd)[col.name]
355   mdesc.sd <- subset.m (data = mdesc.sd)
356   mdesc.sd <- as.matrix (mdesc.sd)
357
358   mdesc.eff.list[[i]] <- mdesc.eff
359   mdesc.sd.list[[i]] <- mdesc.sd
360 }
361
362 mcolor.eff.list <- list()
363
364 maxCFU <- 0
365 minCFU <- -3
366 maxBiomass <- 110
367 minBiomass <- 50
368
369 for (i in sCFU){
370   desc.eff.list[[i]]$effect[
371     desc.eff.list[[i]]$effect > maxCFU] <- maxCFU
372   desc.eff.list[[i]]$effect[
373     desc.eff.list[[i]]$effect < minCFU] <- minCFU
374   color.eff <- rbind(desc.eff.list[[i]], c(10,10,maxCFU),
375                     c(10,10,minCFU))
376   color.eff$effect <- color.scale(color.eff$effect, alpha = 0.5,
377                                  extremes = c("black","white"))
378   color.eff <- color.eff[1:nrow(desc.eff.list[[i])],]
379
380   mcolor.eff <- reshape(color.eff, direction = "wide",
381                         idvar = "d2", timevar = "d1")
382   rownames(mcolor.eff) <- mcolor.eff$d2
383   mcolor.eff$d2 <- NULL
384   colnames(mcolor.eff) <- unique(color.eff$d1)
385   mcolor.eff <- as.data.frame(mcolor.eff)
386   mcolor.eff <- subset(mcolor.eff)[col.name]
387   mcolor.eff <- subset.m (data = mcolor.eff)
388   mcolor.eff <- as.matrix (mcolor.eff)
389
390   mcolor.eff.list[[i]] <- mcolor.eff
391 }
392 for (i in sBiomass){

```

```

393 desc.eff.list[[i]]$effect[
394     desc.eff.list[[i]]$effect > maxBiomass] <- maxBiomass
395 desc.eff.list[[i]]$effect[
396     desc.eff.list[[i]]$effect < minBiomass] <- minBiomass
397 color.eff <- rbind(desc.eff.list[[i]], c(10,10,maxBiomass),
398                   c(10,10,minBiomass))
399 color.eff$effect <- color.scale(color.eff$effect, alpha = 0.5,
400                               extremes = c("black","white"))
401 color.eff <- color.eff[1:nrow(desc.eff.list[[i])],]
402
403 mcolor.eff <- reshape(color.eff, direction = "wide",
404                      idvar = "d2", timevar = "d1")
405 rownames(mcolor.eff) <- mcolor.eff$d2
406 mcolor.eff$d2 <- NULL
407 colnames(mcolor.eff) <- unique(color.eff$d1)
408 mcolor.eff <- as.data.frame(mcolor.eff)
409 mcolor.eff <- subset(mcolor.eff)[col.name]
410 mcolor.eff <- subset.m (data = mcolor.eff)
411 mcolor.eff <- as.matrix (mcolor.eff)
412
413 mcolor.eff.list[[i]] <- mcolor.eff
414 }
415
416 mHSA.syn.list <- list()
417
418 for (i in seq_len(nExp)){
419   HSA.syn.list[[i]]$call <- as.character(HSA.syn.list[[i]]$call)
420   HSA.syn.list[[i]]$call[HSA.syn.list[[i]]$call == "*"] <- cor.syn
421   HSA.syn.list[[i]]$call[HSA.syn.list[[i]]$call == "a"] <- cor.ant
422   HSA.syn.list[[i]]$call[is.na(HSA.syn.list[[i]]$call)] <- cor.add
423   temp <- subset.mono(data = desc.eff.list[[i]])
424   temp$call <- cor.mono
425   HSA.syn.list[[i]] <- rbind(temp, HSA.syn.list[[i]])
426   mHSA.syn <- reshape(HSA.syn.list[[i]], direction = "wide",
427                      idvar = "d2", timevar = "d1")
428   rownames(mHSA.syn) <- mHSA.syn$d2
429   mHSA.syn$d2 <- NULL
430   colnames(mHSA.syn) <- unique(desc.eff.list[[i]]$d1)
431   mHSA.syn <- as.data.frame(mHSA.syn)
432   mHSA.syn <- subset(mHSA.syn)[col.name]
433   mHSA.syn <- subset.m (data = mHSA.syn)
434   mHSA.syn <- as.matrix (mHSA.syn)
435
436   mHSA.syn.list[[i]] <- mHSA.syn
437 }
438
439 dir.create ("Summary_graphs_HSA")
440
441 tiff(filename = paste0("Summary_graphs_HSA/Summary_",
442                       a1,a2,"_HSA_%02d.tiff"))
443 for (i in sCFU){
444   color2D.matplot(mdesc.eff.list[[i]],
445                  cellcolors = mcolor.eff.list[[i]],
446                  show.values = 2, vcol = mHSA.syn.list[[i]],
447                  vcex = 2.5,
448                  xlab = paste(a1,"(mg/L)"),
449                  ylab = paste(a2,"(mg/L)"), yrev = FALSE,
450                  #main = title.list[[i]],
451                  axes = FALSE, border = NA)
452   axis(1,at=0.5:3.5,labels = c(colnames(mdesc.eff.list[[i]])),
453        font = 2)
454   axis(2,at=0.5:3.5,labels = c(rownames(mdesc.eff.list[[i]])),
455        font = 2)
456
457   addtable2plot(0,-0.3,table = mdesc.sd.list[[i]][nrow(
458     mdesc.sd.list[[i]]):1,],
459                bg = "transparent", cex = 1.9,
460                display.colnames = FALSE, ypad = 3.8, xpad = 0.68,
461                xjust = 0, yjust = 1)
462 }
463 for (i in sBiomass){
464   color2D.matplot(mdesc.eff.list[[i]],
465                  cellcolors = mcolor.eff.list[[i]],
466                  show.values = TRUE, vcol = mHSA.syn.list[[i]],
467                  vcex = 2.5,
468                  xlab = paste(a1,"(mg/L)"),
469                  ylab = paste(a2,"(mg/L)"), yrev = FALSE,

```

```

470         #main = title.list[[i]],
471         axes = FALSE, border = NA)
472     axis(1,at=0.5:3.5,labels = c(colnames(mdesc.eff.list[[i]])),
473         font = 2)
474     axis(2,at=0.5:3.5,labels = c(rownames(mdesc.eff.list[[i]])),
475         font = 2)
476
477     addtable2plot(0,-0.3,table = mdesc.sd.list[[i]][nrow(
478         mdesc.sd.list[[i]]):1,],
479         bg = "transparent", cex = 1.9,
480         display.colnames = FALSE, ypad = 3.8, xpad = 0.68,
481         xjust = 0, yjust = 1)
482 }
483 dev.off()
484
485 ### Relationship of elements #####
486
487 ## Data (relevant)
488
489 ## data.list: list of dataframes with results per experiment.
490 ## desc.eff.list: list of dataframes with average results per experiment.
491 ## desc.sd.list: list of dataframes with sd results per experiment.
492 ## fit.data.list: list of output of fitMarginals() per experiment.
493 ## HSA.list: list of output of fitSurface() for hsa per experiment.
494 ## HSA.syn.list: list of dataframes with synergy/antagonism coded by
495 ##               colours for hsa per experiment.
496 ## id.results: dataframe with summary of experiments and acronyms.
497 ## mcolor.eff.list: list of matrix with gradient colors depending on
498 ##               average results per experiment.
499 ## mdesc.eff.list: list of matrix with average results per experiment.
500 ## mdesc.sd.list: list of matrix with sd results per experiment.
501 ## mHSA.eff.sd.syn.list: list of dataframes with pasted average, sd, and
502 ##               synergy/antagonism for HSA per experiment.
503 ## mHSA.syn.list: list of matrix with synergy/antagonism coded by
504 ##               colours for hsa per experiment.
505 ## plot.fit.data.list: list of graphs with marginal fit per experiment.
506 ## results.comb: dataframe with input of results.
507 ## title.list: list of characters with acronyms for titles.
508
509 ## Values that need to be introduced
510
511 ## a1: compound 1.
512 ## a2: compound 2.
513 ## cor.add: color for additivity.
514 ## cor.ant: color for antagonism.
515 ## cor.mono: color for monotherapy.
516 ## cor.syn: color for synergy.
517 ## maxBiomass and minBiomass: maximal and minimal for the range of the
518 ##               color for biomass graphs.
519 ## maxCFU and minCFU: maximal and minimal for the range of the
520 ##               color for cfu graphs.
521
522 ## Functions
523
524 ## check.syn: prints a code for synergies or antagonisms for a single
525 ##               combination from the output of a fitSurface() converted
526 ##               to dataframe.
527 ## define.add: prints NA in the place of "None" or prints the existing
528 ##               value when it is different.
529 ## paste.noNA: merge two columns without adding NA data.
530 ## subset.data: select the columns "d1", "d2" and "effect" from a single
531 ##               "experiment" in a dataframe.
532 ## subset.m: selects rows that do not have NA values.
533 ## subset.mono: selects combinations of "d1" an "d2" that include at least
534 ##               a 0 (zero) value.
535 ## subset.name: selects combinations of "d1" an "d2" that do not include
536 ##               0 (zero) values.
537

```

538 **References:**

- 539 1. Prażyńska M, Gospodarek-Komkowska E. 2019. Paradoxical growth effect of
540 caspofungin on *Candida* spp. sessile cells not only at high drug concentrations. *J*
541 *Antibiot (Tokyo)* 72:86–92.
- 542 2. Shields RK, Nguyen MH, Du C, Press E, Cheng S, Clancy CJ. 2011. Paradoxical
543 effect of caspofungin against *Candida* bloodstream isolates is mediated by multiple
544 pathways but eliminated in human serum. *Antimicrob Agents Chemother*
545 55:2641–7.
- 546 3. Wiederhold NP, Kontoyiannis DP, Prince RA, Lewis RE. 2005. Attenuation of the
547 Activity of Caspofungin at High Concentrations against *Candida albicans*: Possible
548 Role of Cell Wall Integrity and Calcineurin Pathways. *Antimicrob Agents*
549 *Chemother* 49:5146–5148.
- 550